Damage Severity Assessment in Ductile and Brittle Media Using Improved *b* Value Analysis of AE Data

A Dissertation submitted
In partial fulfillment of the requirements
for the degree of

Master of Engineering

in

CAD/CAM Engineering

by

Amit Sharma

Roll No.: 801381003

Under the supervision of

Dr. Sandeep Kumar Sharma

Assistant Professor, MED

MECHANICAL ENGINEERING DEPARTMENT

THAPAR UNIVERSITY, PATIALA

July, 2015

CERTIFICATE

This is to certify that the thesis entitled "**Damage Severity Assessment in Ductile and Brittle Media Using Improved *b* Value Analysis of AE Data**" is an authentic record of my own work carried out as requirements for the award of degree of **Master of Engineering** in **CAD/CAM** at **Thapar University, Patiala**, under the supervision of **Dr. Sandeep Kumar Sharma,** Assistant Professor, Mechanical Engineering Department, Thapar University during July, 2013 to July, 2015. No part of the matter embodied in this report has been submitted to any other university or institute for the award of any degree.

Date: July 14, 2015

(Amit Sharma)
Reg. No. 801381003

It is certified that the above statement made by the student is correct to the best of my knowledge and belief:

(Dr. Sandeep Kumar Sharma)
Mechanical Engineering Department
Thapar University, Patiala - 147004

Countersigned by:

Dr. S.K. Mohapatra
Head, Mechanical Engineering Department
Thapar University, Patiala-147004

Dr. S.S. Bhatia
Dean of AcademicAffairs
Thapar University, Patiala-147004

ii

Dedicated to

My parents and friends

Acknowledgement

I am highly grateful to the authorities of Thapar University, Patiala, for providing this opportunity to carry out the thesis work.

I would like to express a deep sense of gratitude and thank profusely to my thesis guide **Dr. Sandeep Kumar Sharma** for his sincere & invaluable guidance and suggestions which inspired me to present thesis report in the present form. I would also like to pay my sincere thanks to Dr. Shruti Sharma, Assistant Professor, CED for guiding me in the casting of concrete specimens. I am highly thankful to **Dr. S.K. Mohapatra, Sr. Professor and Head,** Mechanical Engineering Department for his invaluable guidance & permission to carry out experimental work in the department.

I would like to thank my friends Gaurav Arya, Ashutosh Sharma, Gaurav Sharma, Gurdeep Singh, Sourabh Dwivedi for their invaluable support in organizing the research project.

(Amit Sharma)

Abstract

Non-destructive testing has evolved as one of the most preferred testing method for structural health monitoring. Structural health monitoring in the field of aerospace, mechanical, nuclear power, civil engineering, etc. requires techniques to detect damage at early stages of development. The early detection of damage helps to take appropriate action required for retrofitting. Risks to human lives can be decreased if the time of catastrophic failure is well known. AE is preferred over other NDT techniques for its in-situ examination and for its active nature. Damage quantification tools are used to analyse data to know the type, size and severity of damage. This report presents the use of improved *b* value analysis to differentiate I*b* values for indication of failure mechanisms in ductile and brittle material.

In the present study, mild steel specimens were used as ductile material and concrete cubes cured for different time period were used as brittle material. The mild steel specimens were tested in tensile loading at different loading rate. The R15α sensors were mounted with the help of tape using grease as couplant. In bending, a notch was deliberately machined on tension side in mild steel specimens. In case of concrete, cubes cured for different time period were tested under compressive load. The R3α sensors used for the study of brittle material were mounted with the help of grease and tape. The AE data captured for both ductile and brittle material was analysed using improved *b* value analysis. Amplitude, absolute energy, improved *b* value, load and other parameters were plotted with time to understand failure mechanisms in ductile and brittle materials. The I*b* value for both ductile and brittle material was obtained.

Contents

List of Figures

List of Tables

Chapter 1

Introduction

1.1 Motivation

The process of applying techniques for identification of damage in the field of civil, mechanical and aerospace engineering is known as Structural Health Monitoring (SHM). Damage can be any change in the material, geometric properties of the system, changes in the connectivity and boundary conditions of the system which affects system's performance. For most of the public and private infrastructure systems, it is desirable to detect damage in the early stages of damage initiation. So these organizations require SHM to be performed on their products and infrastructure. Aerospace companies have been employing SHM techniques to identify damage on the control surfaces of space shuttle hidden by heat shields. The practical use of SHM have increased with the development of sensor technology, refined structural concepts and multifunctional materials. Two factors that are considered in SHM are time scale of change which deals with the information of time related to phenomenon of change and other factor is severity of change which deals with the information of degree of change. Two different techniques, global and local techniques are used to monitor the health of structure. Global technique takes into account dynamic characteristics of structure to identify damage, severity and location of damage. So global technique reduces need for manual inspection. Local techniques are used for monitoring mechanical structures [1].

1.2 Structural health monitoring

SHM (Structural Health Monitoring) refers to the operation used to measure the condition of structures, monitoring their performance and to detect damage at early stage. Early damage detection and the prognosis will help to prevent the failure of the structure, saves money on maintenance and to make sure that the structure operates safely for the time it is designed. All systems and components are subjected to cyclic or random loads, environmental exposure. It leads to some degree of deterioration such as wear, cracks and corrosion. In aerospace engineering e.g. the most important problems are corrosion, internal cracks and fatigue in wings and fuselage. Monitoring of structures was not a need in past time as structures were overdesigned. Due to technical and economic reasons the use of excess material has reduced

in earlier time which leads to limited lifetime of the structure. Bridges are one of the important aging infrastructures which need effective SHM tools from the point of their economic significance (as their building cost is high) as well as, bridges directly affect public safety. From the time, bridges were designed there had been many changes in the load pattern. The loads and deterioration with time can create localized distress and if not corrected in time, can cause its failure. Every year a huge amount of money is spent on the maintenance of bridges and buildings in the world. Failure of bridges can cause big loss of money as well as lives for e.g. Kadalundi river rail bridge, India on 21 July 2001 which results in 57 deaths. The bridge was 150 years old and due to its poor state of repair the train derailed and results in loss of so many lives [22]. So from these facts it is clear that early damage detection and appropriate action is necessary to save lives and to achieve economic benefits. Visual Inspection by trained personnel has been a conventional mean of bridge monitoring but it solely can't find all damages for e.g. Crack hidden by paint and crack in areas, hard to reach in visual inspection. Hence it is much needed to have a technique to monitor structural health of engineering structure and give early indication of damage. The reasons SHM is used are

1.2.1 Detection of damage

This is the most important reason behind the use of SHM. The structures are monitored continuously and any change in its system is noted. In aerospace history for e.g. shuttle modal inspection system (SMIS) was developed to describe fatigue damage in various components as fuselage, control and lifting surfaces. The aim is to find damage in its early stages such that preventive actions can be taken before catastrophic failure.

1.2.2 Phenomenon of damage growth

The structures are monitored for a long time to study phenomenon behind the growth of damage. Objectives of studying damage phenomenon are

- Design procedure/processes involved in the manufacturing of the structure can be improved.
- Material selection can be improved.

1.2.3 Functionality

The structures can be monitored to check their functionality. The structures are loaded to the conditions as in real time working. So any flaw if detected can be studied and changes can be done in the initial design and then manufacturing stage.

1.3 Non Destructive Testing (NDT)

NDT (Non-destructive testing) is a set of different techniques used to find discontinuities and characterize properties of materials without causing functional damage to them [2]. It is known by different names as Nondestructive examination (NDE), Nondestructive inspection (NDI) and Nondestructive evaluation (NDE). NDT has been used for many centuries with initial development in instrumentation incited by the advance in technology that came during World War II. During 19^{th} and 20^{th} century big accidents (rail accidents, exploding of boilers etc.) gave a push for the rapid development of NDT. Earlier the primary purpose was detecting flaws or damage in the components. Products were designed to make sure that the products throughout its life do not develop macroscopic damage. To detect damage at earlier stage many techniques like eddy current, magnetic particle etc. were developed. A major change in NDT came in the early 1970's. Components were rejected on the detection of small flaws but it had not changed the probability of component to fail. But with the development of fracture mechanics, it became possible to find whether a component with small defect will fail when loaded to service level loading. Other developments lead to prediction of crack growth under fatigue loading. With these developments it became possible to accept defected components if the size of defect is known. A defected component could be in service as long as the defect would not grow to critical size or size leading to failure. So it became a new challenge in NDT community. Detection of damage solely was not enough. To serve as an input to fracture mechanics it was important to obtain defect size so that the remaining life of product can be calculated. It gave rise to quantitative nondestructive evaluation (QNDE) technique.

1.4 History of NDT

When did NDT come into existence? Some people would answer this question by referring what is being written in Genesis. God created the earth and heavens in the beginning and He saw it was good. This theme has been used for a long time to describe the history of NDT. The visual test (seeing the earth and heavens were good) has been identified as the first nondestructive test. It is difficult to precisely identify when NDT began. In ancient times how

strong the metal of sword would be in combat was judged by the audible rings of a Damascus sword blade. The same technique was used by the blacksmiths for a very long time. They used to listen sounds from the different metals being shaped. Table 1.1 depicted below gives details about the origin and development of NDT techniques

Table 1.1 Origin and development of NDT techniques [3]

Year	Technique	Inventor
BC (appx.)	Visual Testing	God
1800	Thermography	Sir William Herschel
1831	Electromagnetic Induction	Michael Farraday
1840	Infrared Image	John Herschel
1868	Magnetic Particle Testing	S.H Saxby
1879	Eddy Current Testing	E. Hughes
1895	X Rays	Wilhelm Conrad Roentgen
1922	Industrial Radiography	Dr. H.H Lester
1940-1944	Ultrasonic Test Method	Dr. Floyd Firestone
1950	Acoustic Emission	J Kaiser

1.5 Conditions for effective Non Destructive Testing

The following factors associated with NDT can affect NDT in direct or indirect ways. These factors need to be optimized and controlled for an effective NDT. The factors are

1.5.1 Product to be tested

The product to be tested directly affects the type of NDT process used. The geometry and shape of product give rough information about the type of process used for testing. For e.g. a small casting with complex shapes cannot be tested conveniently with Ultrasonic testing. It would be appropriate to use radiography in this case.

1.5.2 Procedure

Proper procedure should be followed in testing products. Procedures vary with respect to the type of detection, availability of sources and the type of specimen. A procedure is approved by an experienced personnel who is highly qualified to properly asses the sufficiency of procedure.

1.5.3 Equipment

The equipment used in testing should operate properly. It should be properly calibrated. Regular checks should be performed to make sure that all the components are operating accurately as it can affect output.

1.5.4 Qualified Personnel

Qualified personnel should carry out testing as their results affects the life of structure. Adequate training should be provided to the testers.

1.6 Destructive versus nondestructive test

The mechanical testing to evaluate quantitatively characteristics of the material is known as destructive testing. In some cases the material is loaded to in-service loading conditions. The precise information obtained from tests are applicable to specimen being examined. The specimen once tested cannot be used subsequently for any application. These tests give useful design information and about life of the product. These tests give information about:-

- Ultimate tensile strength
- Corrosion resistance
- Toughness
- Hardness
- Fatigue life
- Impact resistance
- Yield point
- Ductility
- Elongation characteristics

The advantages of destructive tests are listed as under:

- Accurate and reliable data about the test specimen.
- Useful data for design purposes.
- Standards and specifications can be established.
- Quantitative data is achieved.
- Various service conditions can be measured.
- The life of product can be predicted.

Besides various advantages the disadvantages of destructive tests are listed as under:

- Data applicable to specimen being examined and needs to be generalised.
- Test specimen cannot be used for working purpose.
- Expensive equipment is required.

Non-destructive tests have following advantages as:

- The specimen can be used for working purpose after testing.
- A large portion can be examined without adversely affecting the functioning.
- Surface and internal examination can be effectively carried out.
- In service examination of parts can be done using some of the NDT processes.
- Nondestructive tests are cost effective.

Non-destructive tests have following disadvantages as:

- Results are usually operator dependent.
- Nondestructive tests are cost effective.
- Generally quantitative data.
- Subjective evaluation of some test results can be subjected to dispute.
- Most of the methods are cost effective but some for e.g. radiography can be expensive.
- Defined procedures have to be opted.

Thus, destructive and nondestructive test have some advantages and limitations but when these are used together can give much valuable information about the life of product.

1.7 NDT techniques

All NDT techniques are used to find discontinuities without causing damage to structure or component being examined. NDT techniques like visual and optical testing, electromagnetic and penetrant testing are used for only surface defects while techniques like ultrasonic testing, radiography and acoustic emission testing are used for both surface and buried-in defects. Following are the types of NDT techniques commonly used:

1.7.1 Penetrant Testing

A layer of visible or fluorescent dye solution is coated on the specimen. A developer is applied on the surface after wiping excess dye from the surface. The developer draws penetrant out of

imperfections open to the surface. Intense colour contrast between the developer and penetrant make “bleed out” easy to see.

1.7.2 Visual and optical testing

Visual inspection involves inspection with naked eyes to look for defects. The inspector may also use magnifying glasses or mirrors to inspect more closely the test area.

1.7.3 Eddy current testing or Electromagnetic testing (ET)

An alternating magnetic field is induced in a conductive material. These magnetic fields flow in circle below the surface of the material. Distraction in the flow of eddy currents, caused by dimensional changes, imperfections or changes in the materials permeability and conductive properties, can be detected with the proper equipment.

1.7.4 Magnetic Particle Testing (MT)

Iron particles are sprinkled either in dry or wet form on the surface of the ferromagnetic material. A magnetic field is induced in the material. Iron particles concentrate near surface defects as magnetic field is distorted by the discontinuities. Then through visual inspection flaw can be detected.

1.7.5 Leak Testing (LT)

Various techniques are used to detect and locate leaks in pressure containment parts, structures and pressure vessels. Liquid and gas Penetrant techniques Electronic listening devices, pressure gauge measurements, and/or a simple soap-bubble test are used to detect leaks.

1.7.6 Ultrasonic Testing (UT)

High-frequency sound waves are transmitted into a material to detect imperfections or to locate changes in material properties. Pulse echo and Pulse transmission are the most commonly used ultrasonic testing technique. In pulse echo technique sound is introduced into the specimen and reflections (echoes) from internal imperfections are returned to a receiver.

1.7.7 X-Ray fluorescence

Radioactive sources or a low voltage x-ray generator acts as a source of radiation. Energy is generated as element specific radiation is sent back. The reflection generates different energy level for each element as elements have different atomic structure. Alloy elements are

identified by measuring energy. The dimensional features of the part are shown in the shadowgraph. Density change on the film is the measure of imperfections in the same manner as broken bones are shown by medical X-ray.

1.7.8 Infrared Thermography

It does not affect any ongoing process and calculates the temperature difference ranging from -50˚C to 1500˚C. Thermo graphic camera detects temperature across complete surface.

1.7.9 Acoustic Emission Testing

Acoustic emission is defined as the range of phenomena that results in the generation of structure-borne and fluid-borne (liquid, gas) propagating waves due to the rapid release of energy from localized sources within and/or on the surface of a material. When external stimulus for e.g. load, change in pressure, temperature is subjected to a structure then there is a release of energy by localized sources i.e. defect sites. This energy is in the form of stress waves that travel to the surface and are recorded by sensors.

1.8 Comparison between NDT techniques

Various NDT techniques have developed with time. The process to be selected for testing purpose depends on various factors as accuracy, cost of inspection and other factors. Accuracy plays a vital role in the selection of NDT process. The testing process should be capable of detecting defects smaller than defects leading to failure. So it is much important to have a basic understanding of parameters based on which a process is selected. Table 2.2 depicted below gives a comparative analysis between different NDT processes.

Table 1.2 Comparative analyses of NDT techniques [2]

Method	Application	Advantages	Limitation
Penetrant Testing	Any nonabsorbent solid material having uncoated and uncontaminated surfaces.	Easy to use. Inexpensive. Versatile and sensitive. Minimum training.	Require uncontaminated surfaces. Surface defects can be detected.

Visual and Optical Testing	In service inspection. Raw material and finished products.	Simple and inexpensive. Minimum training required.	Surface defects can be detected. Good illumination source required. Not effective in hard to reach areas.
Eddy current Testing	All conductive materials examined for damage, thinning, metallurgical conditions and conductivity.	Quick. In-situ examination. Noncontacting. Flexible to automation.	Good knowledge of variables required. Only conductive materials required.
Magnetic Particle Testing	All ferromagnetic materials for surface and subsurface discontinuities.	Easy to use. Inexpensive. Highly sensitive. Very fast.	Detection of surface and subsurface discontinuities only. Ferromagnetic materials required.
Ultrasonic Testing	Most materials can be tested	Type, size, thickness, information of defect can be obtained. Precise results.	Good surface finish required to avoid attenuation. Requires couplant.

Radiography Technique	Most materials either in-service or manufactured can be examined	Provides permanent record. High sensitivity. Mostly used volumetric inspection method	Limited thickness can be tested based on material density. Adverse effects of radiation.
Infrared Thermography	Most materials and components can be examined	Provides permanent records. Highly sensitive to temperature change.	High skill required for evaluation. Limited thickness can be tested. Only surface defects can be detected.
Acoustic Emission Testing	Rotating equipment, aerospace, welds etc.	Large areas can be examined. Predict failure of material	Analysis of signal is required. Expensive process. Sensors should have good contact with the surface.

1.9 Concluding remarks

This chapter gives a background of NDT techniques for monitoring health of the structure. SHM is required in various fields such as aerospace, nuclear, civil, mechanical etc. for economic and development purpose. SHM is also required for the safety of human lives as big accidents (collapse of bridges, exploding of boilers) directly affect human lives. NDT techniques have made it easy to find discontinuities in the earlier stages of failure mechanism. Various NDT techniques have been discussed with their advantages and limitations.

Chapter 2

AE-An Important NDT Tool

2.1 Introduction

Acoustic means *akoustikos* in greek words means hearing. For many years sounds are the precursor to structural collapse which are emitted before failure of the structure. A branch of the tree emits sounds before it completely detach from the tree. As visual inspection is to eyes similarly acoustic emission is to ears. Acoustic emission (AE) technique has become one of the most important NDT processes to find defects in mechanical loaded structures or components. A sudden redistribution of stress generate transient elastic waves in a material and referred as Acoustic Emission. When external stimulus for e.g. load, change in pressure, temperature is subjected to a structure then there is a release of energy by internal sources. This energy in the form of waves being recorded by sensors at surface. Energy being concerted to electric voltage is processed as AE signal data with the help of timing circuits. The received signal then is characterized according to frequency, voltage intensity and source location. The main difference between AE technique and other NDT techniques is that it is a passive method. AE frequencies are in the range of 150-300 kHz. The various sources of AE waves are:-

- Slip and dislocation movements.
- Crack initiation and growth.
- Twinning
- Melting
- Phase deformation in metals
- Earthquakes etc.

Figure 2.1 shows how stress waves generate and travel to surface.

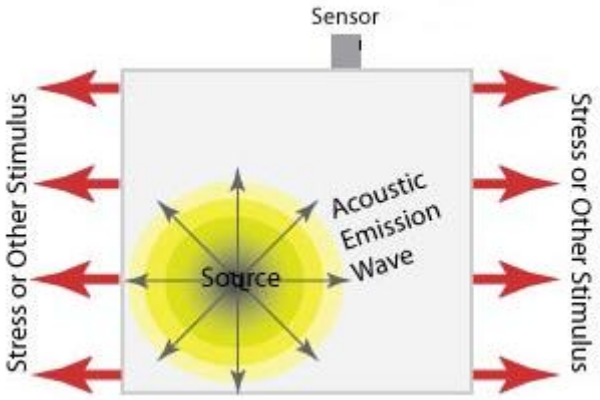

Fig. 2.1 Generation and propagation of stress wave [1]

At some places local stress is high enough to produce new, permanent deformation. Material generate stress waves at these places. Mostly this happens at stress concentrations. It is a location where stress is generated. Stress concentration exist at:-

1. Structural Discontinuity.
2. Changes in section.
3. Crack and flaws.

As metal deform it lead to high local stresses relieved due to deformation. Often load is transferred to other parts of member or structure. This creates stabilization effect. When load is repeated at same level then the other part which was deformed earlier will stabilize this time. Thus there will be no emission till the time load is exceeded.

2.2 History of AE testing:-

Earlier in the history major efforts were put at getting fundamentals of AE phenomena and how AE behaves during fracture and deformation inside material. The origin of AE is hard to find as this can occur naturally. There are different facts about their first working appearance and publication of works.

Around 6500 BC potters used to find structural failure of their pots by listening sounds during cooling of ceramics. Around 3700 BC tin smelters in Asia Minor coined “tin cry”.

J.E Kaiser carried out AE on metals in Germany in 1950. Kaiser discovered that no acoustic emission will appear unless the previously applied load on the member is exceeded and is

known as Kaiser Effect. In terms of terminology the use of AE was started by B.H Schofield in the US in 1954. He published a report entitled “Acoustic Emission under Applied Stress”. Drouillard reported that first report on AE experiment was published in Japan.

Ohtsu *et. al* reported that the first publication was reported in 8th century by Jabir ibn Hayyan. He wrote that iron ‘sounds much’ when forged and tin gives a ‘harsh sound’ when worked. Scruby *et. al* reported that the first physical application of A.E was the testing of rocket-motor casing in 1964. The first application of AE monitoring on bridges was proof testing of a portable military tank bridge. So first application of AE cannot be clearly defined.

2.3 Features of AE signal

Following are the important parameters as related to the AE data recorded by AE sensors

2.3.1 Hit

Hit is the process of detection and measurement of an AE signal on an individual sensor channel.

2.3.2 Event

Event causes numerous hits . A single event can be detected on multiple sensors.

2.3.3 Amplitude (A)

It is the maximum value of the waveform which is recorded by the sensors. It is one of the important parameter used in this study. It is an important parameter because for AE signal, its amplitude value should cross a predefined amplitude for detection of signal. It is measured in dB_{AE}. At the input of preamplifier, a decibel scale running from 0 to 100 dB_{AE} is defined as an amplitude of one microvolt.

2.3.4 Rise Time (R)

The time between the first value which passes threshold and the amplitude is known as rise time.

2.3.5 Duration (D)

The time difference between first and last signal which passes the threshold limit is known as duration. It is measured in microseconds. The relationship between amplitude and duration tells about the signal's shape.

2.3.6 Marse (E)

It defines the area under the voltage time graph of the signal generated by the sensor. Under loading when a structure emits many waves then the total amplitude can be produced by adding energies of individual signals. It is showed in Fig. 2.2

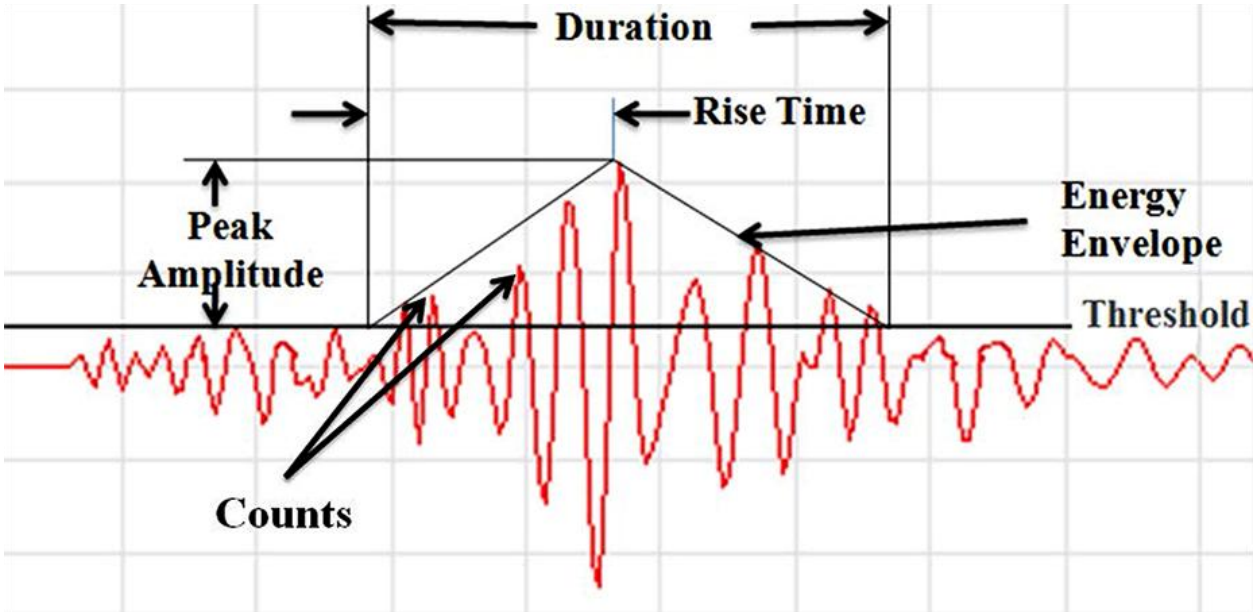

Fig. 2.2 Signal Parameters [2]

2.3.7 Counts (N)

Counts are defined as the number of signals which crosses threshold and are recorded by the sensors. A single hit can produce one count or many counts depending upon the type of signal. In the early years, counts were the most important parameter to describe AE quantity. During 1980's counts were replaced by energy as measure of AE activity. It is considered along with other parameters (amplitude and duration) to give a relevant information.

2.4 Equipment used in AE technique

AE technique can be applied in laboratories and also in field examinations. A typical AE system includes following components

2.4.1 Sensors

AE event cause dynamic motions which is recorded by the sensors. Mechanical movement is being converted to voltage by piezoelectric crystal. Figure 2.3 shows different type of AE sensors.

Fig. 2.3 Different AE sensors

The sensors are selected on the basis of operating conditions, specimen under examination, environment conditions etc.

2.4.2 Preamplifiers

It is an electronic amplifier which prepares small electric signals for further processing or amplification. To avoid noise and interference preamplifiers are placed closed to sensors. Figure 2.4 shows preamplifiers used in AE examination. Many transducers today are integrated with preamplifiers. Amplifiers are used to boost signal strength.

Fig. 2.4 Voltage Preamplifier

2.4.3 Filters

A band-pass filter passes or rejects frequencies with respect to an operating range. The various filters are as:

- **Active band-pass filter**
  The filters which require external power and consist of integrated circuits and transistors.
- **Passive band-pass filter**
  The filters which don not require external power and consists of passive components such as inductors and capacitors.

Filters ignores unwanted signals and optimizes the sensitivity of receiver.

2.4.4 Amplifiers

It is an electronic instrument which increases the power of the signal. It makes the output signal stronger than input signal. Voltage, transconductance, current, transresistance amplifiers are four basic types of amplifiers.

2.4.5 Storage Equipment

Computers or similar devices are used for storage purpose. Figure 2.5 shows storage device used in AE examination.

Fig. 2.5 Storage device used in AE technique

2.5 AE Sources

During the transformational phase change from elastic to plastic then the noticeable acoustic emission takes place. Through the movement of dislocation, the atomic planes slip past each other, as plastic deformation occurs. These deformations release energy and act as a source of AE. In case of cracks the stress in front of crack tip is much higher than the stress at the

surrounding area. So whenever there is a plastic deformation ahead of crack tip, Acoustic emissions are generated.

Fatigue cracks also generate AE. There are two sources of AE in case of fatigue cracks.

- Emissive Particles at the origin of crack tip are the first source of AE in case of fatigue cracks. They are less ductile as compared to surrounding material and break more easily giving acoustic emissions.
- Extension of crack tip happens due to dislocations and triaxial stresses and results into acoustic emission.

2.6 Advantages over other NDT techniques

AE technique now has been emerged as a much used NDT technique. The areas covered under AE technique are much wide. The salient features which make AE better than other NDT techniques.

- In AE technique there is no need to supply energy to the component under consideration. Energy is released by the source itself. Whereas in other NDT techniques we need to supply external energy to find defects. e.g. ultrasonic testing, x-ray testing.
- Real time monitoring also discriminate AE from other NDT sources. This make AE is a useful application as we don't need to stop working of a system or component under consideration.
- It deals with dynamic changes. It means only active cracks or defects are considered.
- In AE technique there is no need to clean the sample.
- Using multiple sensors fast volumetric inspection can be carried out.
- System purchased once can be used multiple times instead of purchasing again like in other NDT techniques.

2.7 Limitation of AE technique

AE techniques also has certain limitation. In spite of many good features there are places where it is not feasible to apply AE technique. The limitations of AE technique are

- A lot of data is generated during AE testing which is difficult to analyze.
- Some defects go unnoticed if the loading limits doesn't exceed the previous loading condition as AE technique takes into account active defects.

- A skilled personnel is needed to deal with AE monitoring and analyzing data.
- It is difficult to have accurate data in a much noisy place.
- For global monitoring a lot of sensors are required which make it a complex system of wires, sensors etc.
- The setup used for monitoring had not been designed indigenously so it has to be imported.
- The setup is costlier and need care in handling.

2.8 Difference from other NDT technique

So the table depicted below give an overview of how AE technique and other NDT technique are different to each other.

Table 2.1 Comparison between AE and other NDT techniques

S No.	AE Technique	Other NDT Techniques
1.	Detects movement of defects	Detects geometric forms of defects
2.	Requires stress	Do not requires stress
3.	More material sensitive	Less material sensitive
4.	Less geometric sensitive	More geometric sensitive
5.	Less intrusive on Plant/ process	More intrusive on plant/process
6.	Requires access only at sensors	Requires access to whole area of inspection
7.	Tests whole structure at once	Scan local regions in sequence
8.	Main problem: noise related	Main problem: geometry related

2.9 Applications of AE

AE has been successfully applied for many years in various fields such as mechanical, civil, aerospace etc. AE techniques are used to ascertain soundness of the subject specimen. If there are some damages or defects detected, then to effectively judge their severity and location in the structure being investigated. Some of the examples where criticality of the structure or component is of paramount importance includes aviation sector, nuclear power, heavy oil structures, cross country pipelines etc. Other applications of AE are

- Rocket motor and railroad tank car testing.

- Inspection and quality affirmation, (e.g. scratch tests).
- Glass-fiber reinforced components
- Explore materials
- Leakage test
- Detecting and locating partial discharges in transformers.

2.10 Concluding remarks

AE has emerged as much used NDT technique. AE has lots of potential for accurate detection of damage. It offers various advantages over other NDT techniques but also has some limitations. AE has been applied successfully in every industry and a lot of researchers are contributing towards new modifications or applications in this technique.

Chapter 3

Literature Review

3.1 Introduction

NDT has evolved as the most preferred techniques for the monitoring of structures in the field of civil, mechanical, aerospace etc. For its nondestructive nature NDT has been employed in manufacturing industries. NDT development with time has brought economic as well as human life related benefits. AE, a NDT technique, also been preferred over other NDT techniques has evolved in a very short span of time and research works are being performed for further improvements. Various researchers had worked in the field of AE testing. A brief review of the work carried out in this area is explained in this section.

Wang *et. al* [1982] detected quality of friction welds using acoustic emission. Acoustic emission counts were measured to correlate the weld strength over various process conditions. Flywheel inertia type welding machine was taken for welding purpose. The welding machine was operated with hydraulic motor having speed of 4500 rpm. Dunegan/Endevco model 3000 system was used for acoustic analysis. Two sets of work piece were taken as shown in figure 3.1

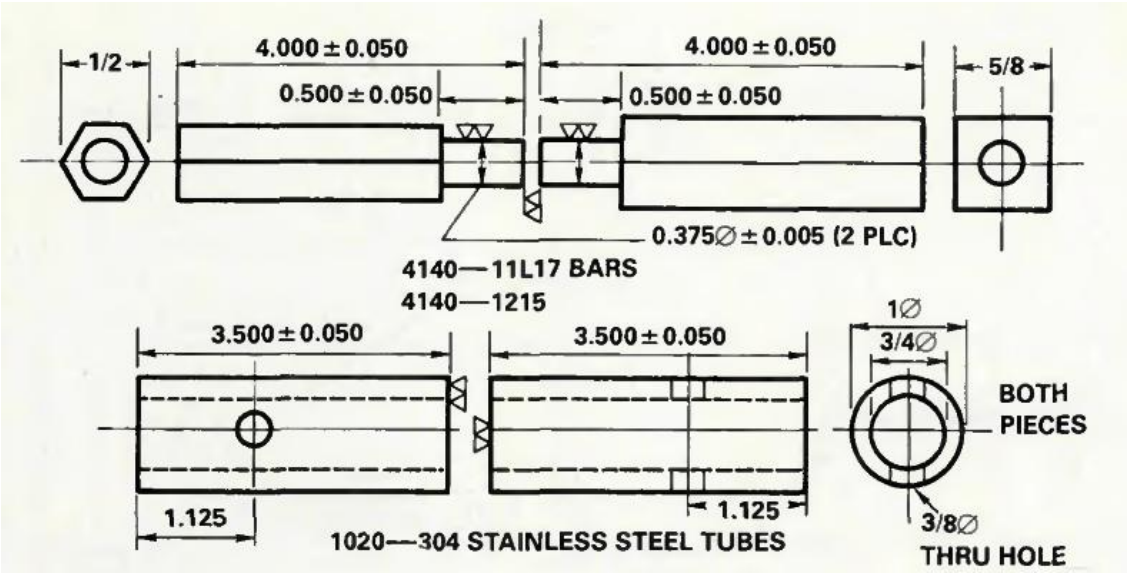

Fig. 3.1 Specimens taken for welds

The hexagonal shape was taken to avoid slipping which could cause additional acoustic emissions. The square shape was taken so that sensors could be easily mounted. 200 samples were made. Six grades of carbon and alloy steel also were used to make work pieces keeping carbon content from 0.08% to 0.38%. Aluminum and copper also were introduced to have differentiation of events produced in ferrous and nonferrous material. Quenching experiments also were carried out on six ferrous and two nonferrous materials. Specimens were heated to 900˚C and were quenched in air, water and oil to find the effect of different cooling rates. It was found that there were two distinctive burst of acoustic emission in case of friction welding of ferrous metals. First burst occurred during welding and second burst occurred after completion of welding. First burst corresponded to the plastic deformation of metal whereas second burst corresponded to the martensitic transformation.

Scruby *et. al* [1987] compiled brief introduction of acoustic emission. Events taken placed inside a solid material were picked by two or more sensors. Three application areas on the basis of source of high frequency sound were reported. They were process monitoring, structural testing, surveillance and material characterization. In the 1st area a defect acts as a source which upon propagation radiates waves. The second area includes examination of manufacturing processes in the materials. The third area was about material research and development. The areas under which AE had come as a useful application were Material Degradation, Reversible processes, Leak and flow, Fabrication Processes. As many processes had the tendency to generate acoustic emissions but which had to be considered was the main issue. So researchers investigated that the localized spatial sources of sound which lie in normal bandwidth i.e. above 20 KHz were ultrasonic. In case of brittle crack waves having high amplitude take away large fraction of energy from the source. But in case of ductile crack the energy moved to drive dislocation in the enlarged plastic zone. Thus it helped in presenting the progress of crack. Figure 3.2 shows that the tip of the crack was blunt. Instead of energy it was the energy release that controls the amplitude of AE signals. So the growth of brittle cracks should be readily detectable whereas slow ductile cracks were hardly detectable. In case of brittle materials AE could be reactive to very small gain in crack length (≈1μm). For ductile materials AE could be insensitive to large crack advances.

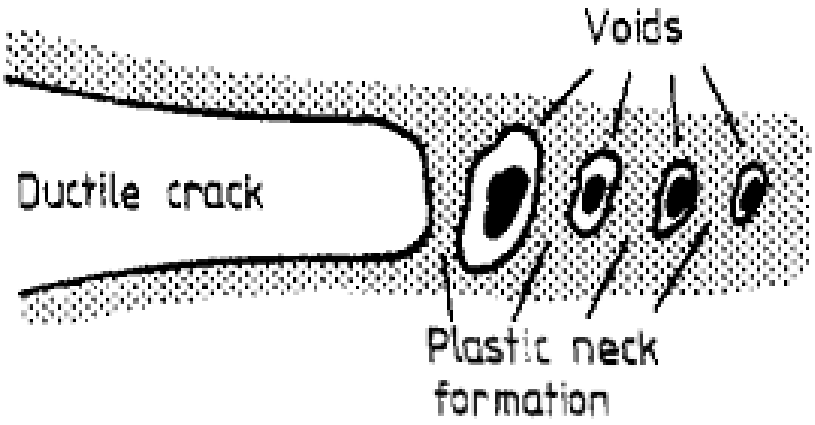

Fig. 3.2 Blunt shape in case of ductile material

Ohtsu *et. al* [1994] compiled the history and development of AE in concrete engineering. Authors listed the contribution of J Kaiser in 1950 to evaluate the state of health of metals. In 1954 B.H Scofield initiated the use of AE terminology in USA. Recently T.F Drouillard found that first report on an experiment carried out with the help of AE was published in Japan. At the time of fracture the stored strain energy was released. Some part of the energy was released as stress waves and were known as acoustic emission. AE signals were amplified by pre-amplifier and main amplifier respectively. Elastic vibrations of 10^{-9} mm were transformed into 10^{-6} V by a typical sensor. In concrete the AE events were detected with the help of amplifier of 60 to 100 dB of gain.AE research had shifted to application age from development age in civil engineering. In case of practical problems AE had not been successful every time, so further studies were needed.

Finalyson *et. al* [2000] explained the use of acoustic emission in aerospace field by monitoring health of an aerospace structure. Acoustic Emission-helicopter health and usage monitoring system (AE-HUMS) is used to detect damage in helicopter drive trains. The test data obtained from SH-60 drive train was used to develop this system. It had made possible to find a crack in pinion fifteen minutes prior to its failure. It characterize damage into four levels with the help of four colors. Green indicates no damage, Yellow indicates minor damage which is non progressive, Orange indicate severe damage but non progressive and Red indicate severe damage but it is progressive in nature. Second technique is aircraft full scale fatigue test (FSFT). In this technique the actual fatigue spectrum, which the structure faces during its flight, is taken into account. The aim of this technique is to find fatigue affected regions and repair them in the prepared actual conditions.

Colombo *et. al* [2003] assessed damage for reinforced concrete beam with the help of b-value analysis. b value was derived from Gutenberg and Richter formulae used in seismology. The b value in the field of AE was given by $Log_{10}N=a-b^1 A_{dB}$, where N was the incremental frequency, A_{dB} was the peak amplitude of AE events and a was the empirical constant. The b value was calculated by multiplying b^1 with 20. Author used 2.6 m long beam with a crosssection of 125 mm x 270 mm. The beam was reinforced with 16 mm diameter deformed steel bar. A simply supported beam of span 2 m was loaded at two points. A load with 5 kN steps was applied. Eight PAC R61 sensors were used. During the test the crack were classified with respect to the loading cycles. Cycle 1 had no cracks, cycle 2-5 involved cracks which were forming and the appearance of tensile crack along the span, cycle 6 involved appearance of shear cracks. It was found that lower b value indicates macro crack whereas high b value indicates micro cracks. b value greater than 1 and less than 1.2 indicates that channel was very near to large crack. B value greater than 1.2 and less than 1.7 indicated uniformly distributed cracks. b value greater than 1.7 indicated macro cracks opening.

Drummond *et. al* [2006] studied emissions generated from wire ropes during proof and fatigue testing. Authors used specimens that were made from 10mm steel wire ropes of a configuration of 6x36(14/7+7/7/1) Inner Wire Rope Core. The rope had a breaking load of 72.9kN, a proof load of 25.5kN and a safe working load of 12.75kN. Different damages were seeded in the wire with the help of saw. The acoustic emission signals having five or more than five counts were accepted. In the initial stage proof load was applied several times on the undamaged rope and after that safe working load was applied three times. After that again proof load was applied. The damage was created then with the help of saw and safe working load was applied three times followed by final proof load. Threshold was taken as 40 dB. The qualitative and quantitative nature of the signals were explored and it was found that signals classify the condition of ropes while it is under periodic proof loading. It was found that signals above 80 dB can differentiate between signals relating to damage and non-damage processes.

Kurz *et. al* [2006] studied quantification of stress drop and its distribution in concrete with b and I*b* value analysis. In micro cracking a large number of AE signals were generated so it lead to a higher b value. In case of macro cracking b value was lower .So as the stress increased b value decreased from a higher to a lower value as fracture process shifts from micro to macro cracking. Two parameters were needed in case of b value analysis first being the event number and the magnitude of the event. Authors used beam with a cross section of 150 x 150 x700 mm^3. For reinforcement steel fiber of span 60 mm and of 0.75 diameter mm was introduced.

A notch of depth 33 mm and width 3mm was deliberately inserted in the middle of the beam. Servo hydraulic 100 kN test frame was used for the transmission of force. The lower supports were fixed and kept at a distance of 600mm. The third cylinder was kept in the middle at the top face. A static load of 7.5 kN was applied. Eight sensors were used. The load was increased in the start, middle and end stage of the experiment.

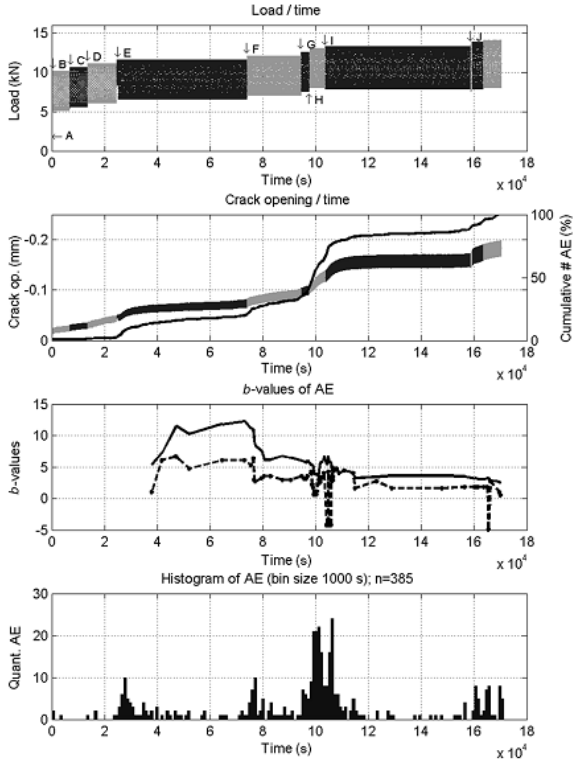

Fig. 3.3 Variation of crack opening, b value and AE signals with time

The crack opening and equivalent AE were plotted with respect to time and it was found that they run parallel to each other thereby indicating that AE activity reflects crack opening. At the start of each loading phase it was found that a large AE signals were accumulated. The I*b* curve had three large minima which coincided with the highest slopes on crack opening curve. It was found that b value was able to find fatigue in the material whereas Ib value gave occurrence of micro cracks.

Loutas *et. al* [2009] compared the results obtained from single stage gearbox monitored with vibration based and AE based technique. Authors used a test rig with two gears (045M15 steel) with pressure angle 20^0, module 3mm and have 25 and 53 teeth. Ball bearing were used to support shafts. Proper lubrication in the setup was ensured. Vibration based and acoustic based processes were applied to monitor gearbox. . The crack had been artificially induced in the gear. Bruel and Kjaer accelerometers were used in vibration based approach. Sampling

frequency of 50 Hz was used and signals having duration of 1s were recorded. Three sensors were used in AE approach. These sensors were mounted on output shaft, bearing of the output shaft and with the input rotating gear. Various parameters from time and frequency domain were calculated for both testing methods. Parameter p_1 denotes the mean of the signal, p_5 is the absolute maximum of the signal, p_4 is the standard deviation of the signal, p_6-p_7 are the third and fourth moments, p_8-p_{11} results from the previous parameters which are calculated by the signal in time domain. P_{12}-p_{24} are calculated in time domain. In case of vibration based approach out of 50 parameters only 12 had the diagnostic potential. In vibration based approach p4, p6, p7, p12, p13, p17, p21, p24, ED1, ED2 and ED3 proved capable of attending the damage accumulation upon the gears. In AE approach p4, p6, p7, p12, p13, p17, p21, p24, ED3, ED4 and ED5 proved capable of attending the damage accumulation upon the gears. It was found that AE technique was more superior in the early and middle stages of crack propagation than vibration based monitoring technique.

Proverbio *et. al* [2009] assessed damage in post tensioned concrete viaduct by b and Ib value analysis. Researchers reported that in brittle failure b value ranged from 1.5 to 2.5 in the initial stages then it decreased to 1. The b value was applied to a group of some events. 100 events were considered to calculate b value. To overcome this problem of making groups improved b value analysis was proposed. 13 and 8 span viaducts with span length of 22m were built in 1956 on the national road number 114 on the eastern coast of Sicily island. A five cell longitudinal trapezoidal void section cross girder characterize each span. Proof loading was applied for testing. In first loading cycle a 30 tons truck load was applied in the middle and 20 tons truck load was applied in the parallel lane and then the truck was allowed to move. In second load cycle two 30 tons truck load was applied followed by 20 tons truck load on the parallel plane followed by 30 tons truck load in the same lane. The trucks were then allowed to leave. It was found that in first loading cycle, b value decreases with increase in load. In second loading cycle b value scatters. It was also found that I*b* value was more sensitive in indicating changes in AE during microcrcaks and copening of cracks. During unloading the increase in the I*b* value was related to shear crack mechanism.

Kaphle *et. al* [2011] investigated damage quantification technique in acoustic emission monitoring. Authors used steel specimen of dimension 300 mm x 25mm x 10 mm. A notch was deliberately inserted in the specimen to initiate crack. INSTRON tensile testing machine was used for the loading rate of 2 mm/min. Three point bending was applied on the specimen. Two R15α sensors were mounted on the ends of the specimen for AE monitoring. The sensors

were mounted with the help of grease and magnetic holders. The threshold was set at 60 dB after pencil lead break test. Loading was stopped after sixteen minutes. I***b*** was calculated for 50 and 75 events and the lowest I*b* was found to be 0.7 about the time of 50s. The lower I*b* value is found in the yielding of specimen.

Gomes *et. al* [2014] evaluated the effect on polyethylene when it came in contact with different fluids with the help of acoustic emission analysis. Polymers were commonly used in fabricating containers used for transporting fluids. Molecular structure of polymer and the manufacturing history of the part decided effect of fluid on polymer. Many factors decided the extent and the rate of sorption of fluid in a polymer. It adversely effects the mechanical properties of the material and could affect the purpose for which that particular polymer was used. So acoustic emission testing hereby was applied to characterize the fluid's plasticizing effect at the time of failure as well as to monitor the polymer when it was in service. Authors used notched test specimens and were immersed fully in sealed container filled with either Igepal solution or Toluene solution and left at ambient temperature to allow soaking for 72 hours. Two AE sensors were used and mounted on same face below and above the notch for monitoring. The third AE sensors was mounted on the mechanical tester to identify mechanical noise. The tensile strength and the ductile nature of the specimens decreased with time. According to acoustic emission analysis the signals having frequency greater than 400 KHz is related to crystalline lamellae damage whereas the signals below 150 KHz indicate inter-lamellae damage.

Haneef *et. al* [2014] studied tensile behavior of AISI type 316 stainless steel using acoustic emission. The chemical composition used to create specimens in terms of weight percentage were Cr/17.1, Ni/12.1, Mn/1.66, Mo/2.4, C/0.04, Si/0.67, Co/0.27, Cu/0.10 and Fe/Balance. Authors used Specimens having dimension of 30 mm x 6 mm x 5 mm annealed at 1273 K for 30 minutes. Specimens were subjected to tensile deformation at strain rates $1.4 \times 10^{-3}\ s^{-1}$, $2.8 \times 10^{-3}\ s^{-1}$, $6.9 \times 10^{-3}\ s^{-1}$ and $1.4 \times 10^{-2}\ s^{-1}$ at ambient temperature. Sensor having resonant frequency 150 kHz, preamplifier with 40dB gain and a band pass filter 100 kHz-300 kHz were used for AE monitoring. Threshold was set at 37dB. It was found that root mean square voltage of acoustic emission increases with increase in strain rate. AE dominant frequency increased with increase in strain rate as velocity of dislocation increases. During necking lower dominant frequencies were observed.

Moustafapour *et. al* [2014] studied acoustic signals due to leakage in the gas pipe theoretically and experimentally. Leakage in buried gas pipe creating vibrations were theoretically analyzed and characteristics of AE signals were analyzed. Authors used steel pipe of radius 130mm, length 6m and thickness 6.4 mm. Two R15a sensors were fixed on the top surface of the pipe for AE monitoring. An opening was created at a distance of 257.8 cm from one end of a pipe. The leakage was allowed through 0.6mm diameter hole. The pipe was buried in a contour of depth 50 cm and sand with a height of 5cm was poured on the pipe. Acquisition system with 16 channel was used. The sampling rate was set at 4 MHz. The operational frequency range was set at 50 to 500 kHz. To find the effect of surrounding medium the experiments were carried out with air-air and air-sand medium. Pipe was filled with air under pressure of 5 bar in both cases. It was found that maximum amplitude and power spectral density of waves was affected by the surrounding medium. In case of air as external medium these two factor have a larger value as compared to sand as surrounding medium. Maximum energy of signals were found near 120 kHz frequency.

Sagar *et. al* [2014] studied the effect of loading rates on reinforced concrete with the help of *b* value analysis. At different loading rates the physical mechanism behind the behavior of concrete under tension was summarized. A reinforced concrete beam was prepared with the dimensions shown in figure 3.4. Loading was applied through four point bending configuration.

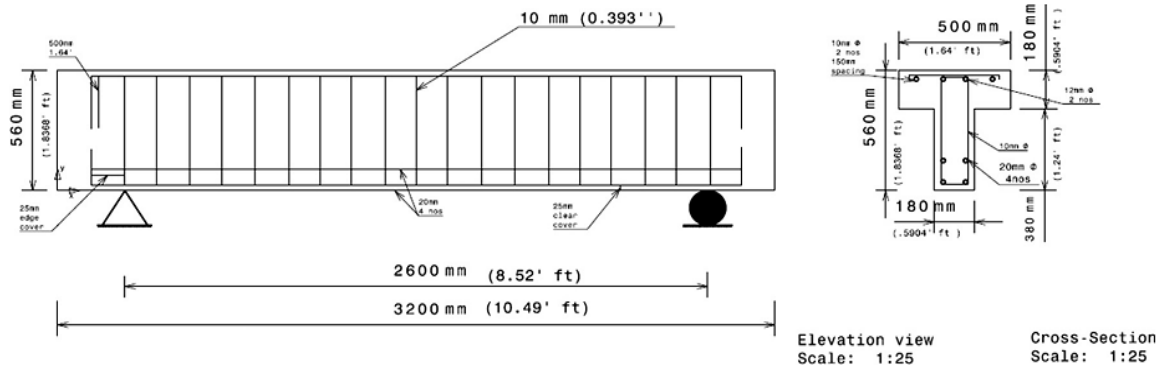

Fig. 3.4 Concrete specimen dimensions

Distance of 1 m was taken as two point loading span and supporting span was kept at 2.6 m. Geometry and reinforcement details are in fig 3.5

Specimen	∅ (mm)	n	A_s (mm²)	S (mm)	L (mm)	Total depth D (mm)	T-beam Flange		T-beam Web(rib)		Rate of loading (kN/s)	Sensor location (mm)											
							Depth (mm)	Width W_f (mm)	Depth (mm)	Width W_{rib} (mm)		1		2		3		5		6		8	
												X	Y	X	Y	X	Y	X	Y	X	Y	X	Y
LC2M37	20	4	1256	2600	3210	560	180	500	380	180	4	460	300	900	240	1600	175	2000	160	2400	210	2800	190
LLR3	20	4	1256	2600	3210	560	180	500	380	180	5	460	300	900	240	1600	200	2000	160	2420	230	2800	200
LLR1	20	4	1256	2600	3210	560	180	500	380	180	6	460	300	900	240	1600	200	2000	160	2400	230	2800	200

Fig. 3.5 Reinforcement details

Φ= Diameter of reinforcing bar

n= number of reinforcing bars

S=span of test beam

L=Total length of test beam

A hydraulic frame of 1200 kN was used along with acoustic emission setup. Loading rates of 4 kN, 5 kN and 6 kN was applied.

The variation of *b* value with different loading rates is shown is figure 3.6

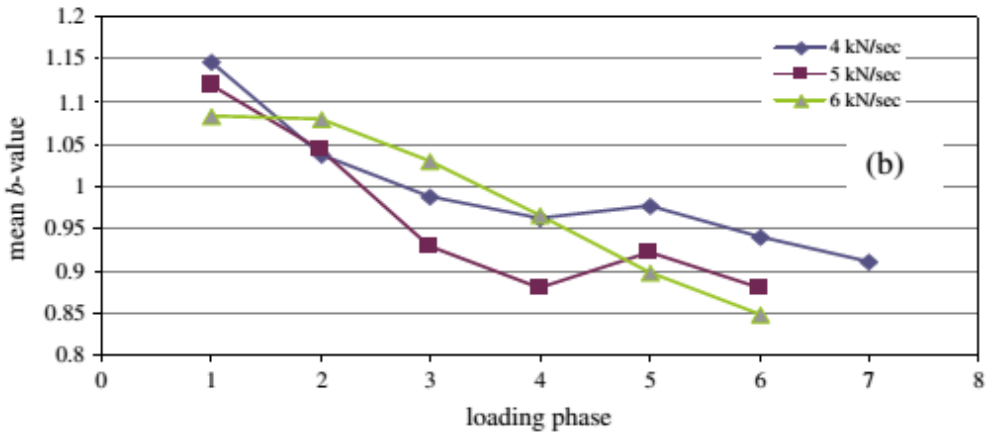

Fig. 3.6 *b* value versus loading rate variation

It was found that with the increase in loading rate there was a drop in *b* value. A sudden drop in *b* value was found with the increase in RA value.

Chen *et. al* [2015] analyzed damage of FRP/Steel composite plates using acoustic emission. Index damage and modified index damage were calculated to analyse damage under cyclic uniaxial loading. Index damage was calculated by cumulative energy at any time divided by cumulative energy when the member experience maximum damage. It was hard to find cumulative energy at the time of maximum damage in practical applications so modified index

damage had been proposed to overcome this limitation. Authors usedf our identical specimens of FRP/steel. The FRP was sandwiched between steel plates. The shape of the specimen is shown in figure 3.7.

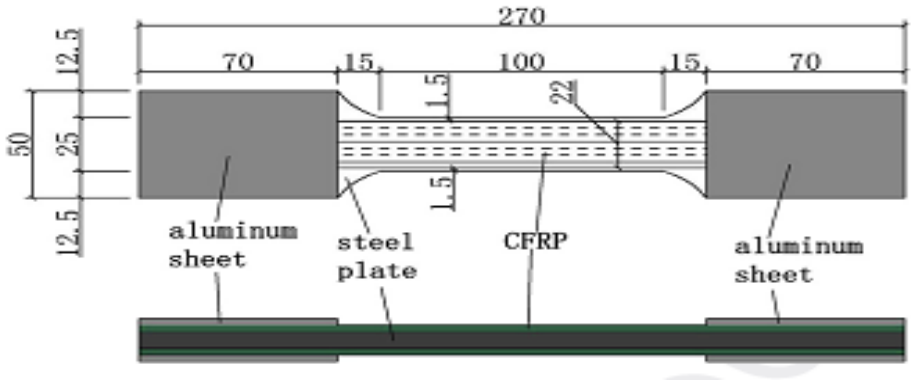

Fig. 3.7 Specimen details

The specimens were tested on universal testing machine. AE sensor was mounted in the middle of the specimen for AE monitoring. The threshold was set at 45 dB, main amplifier gain set at 20 dB and preamplifier gain at 40 dB. The filter frequency was set at 1MHz. The rate of loading was set at 1mm/min. A sentry function was introduced to combine AE and mechanical information. It was defined as the natural logarithm of the ratio between mechanical (strain energy) energy and cumulative energy. It was found that AE energy is steady under uniaxial loading before failure. It was easily to find failure time through AE energy. It was also found that under cyclic uniaxial loading conditions cumulative AE energy increase faster in plastic stage than elastic stage. When index damage was 1 and modified index damage was 1.5 the specimen yields.

Chuluunbat *et. al* [2015] studied influence of loading condition during tensile testing with the help of acoustic emission analysis. Authors used three specimen of aluminum alloy. Instron testing machine was used for tensile loading. Various strain rates $1.25 \times 10^{-4} s^{-1}$, $2.5 \times 10^{-4} s^{-1}$, $1.5 \times 10^{-4} s^{-1}$, $1.25 \times 10^{-3} s^{-1}$ and $2.5 \times 10^{-3} s^{-1}$ were applied on both plain and notched specimen. A 3 mm long and 0.3 mm wide notch was cut with the help of wire cutting. The growth of crack was recorded in the high speed camera. The tensile testing was carried out till fracture happened. The stress strain curve was split into three sections, first up to yield point, second from yield point to peak stress and third beyond peak stress. For non-plain specimen several hits were recorded in the first region. In second region small number of hits were observed. In third region AE activity was stable. The variation between parameters for notched and unnotched specimen is shown in figure 3.8.

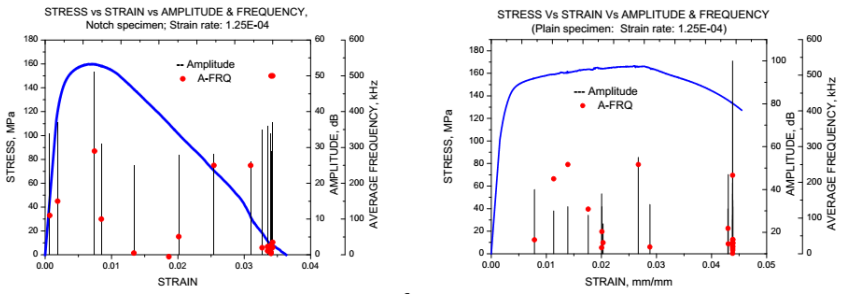

Fig. 3.8 Variation among parameters for notched and plane specimen

Near the end of third region increase in AE hit density leads to the fracture of specimen. It was found that in this region hits having amplitude up to 50 dB and average frequency up to 500 kHz were present. During the testing of plain specimen it showed a different result than notched specimen. In the first region no AE was discovered. In the second region some AE hits appear indicating plastic deformation. Hits having amplitude up to 50 dB and frequency up to 250 kHz were present. In the third region necking was observed followed by the final fracture generating a 100 dB signal.

3.2 Concluding remarks

Various researchers have reported the use of AE an important NDT tool that can be exploited with the following objectives

1. To identify the presence of damage in a structure and adjudge the service worthiness of the structure.
2. To locate accurately and effectively the damage, if any.
3. To identify and distinguish various types of damages by analyzing the recorded AE data.
4. To assess the severity of the damage by quantification of captured AE data.

Chapter 4

Quantification tools for Damage Assessment in AE data

4.1 Introduction

Quantitative analysis of AE data is still hard for applications related to actual structures as standard procedures are not available for all types of structure. Moreover depending upon duration and setup, the data is so voluminous that it is really hard to handle the sheer volume of data. But different parameters quantify the level of damage in AE. These parameters effectively use AE data to quantify the damage in structure.

4.2 Common methods

An index ws developed by Ledeczi. Ledeczi used number of events to measure the activity and intensity. Figure 4.1 shows the index prepared by Ledeczi.

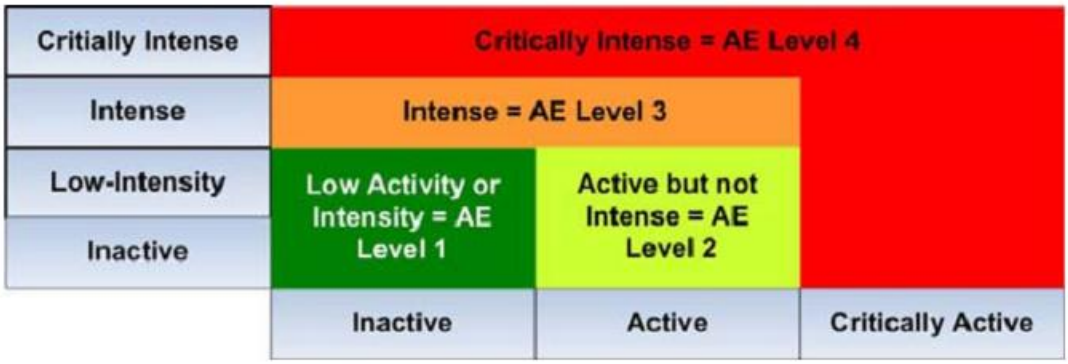

Fig. 4.1 Classification of AE in terms of intensity (vertical) and activity (horizontal)

Crack was categorized into five different levels by Gong using a relationship between stress intensity factor and count rate as

$$N^I = A\ (\Delta K)^n$$

where A and n are constants.

ΔK is the stress intensity factor and N is the count rate

Figure 4.2 shows the relationships between various parameters.

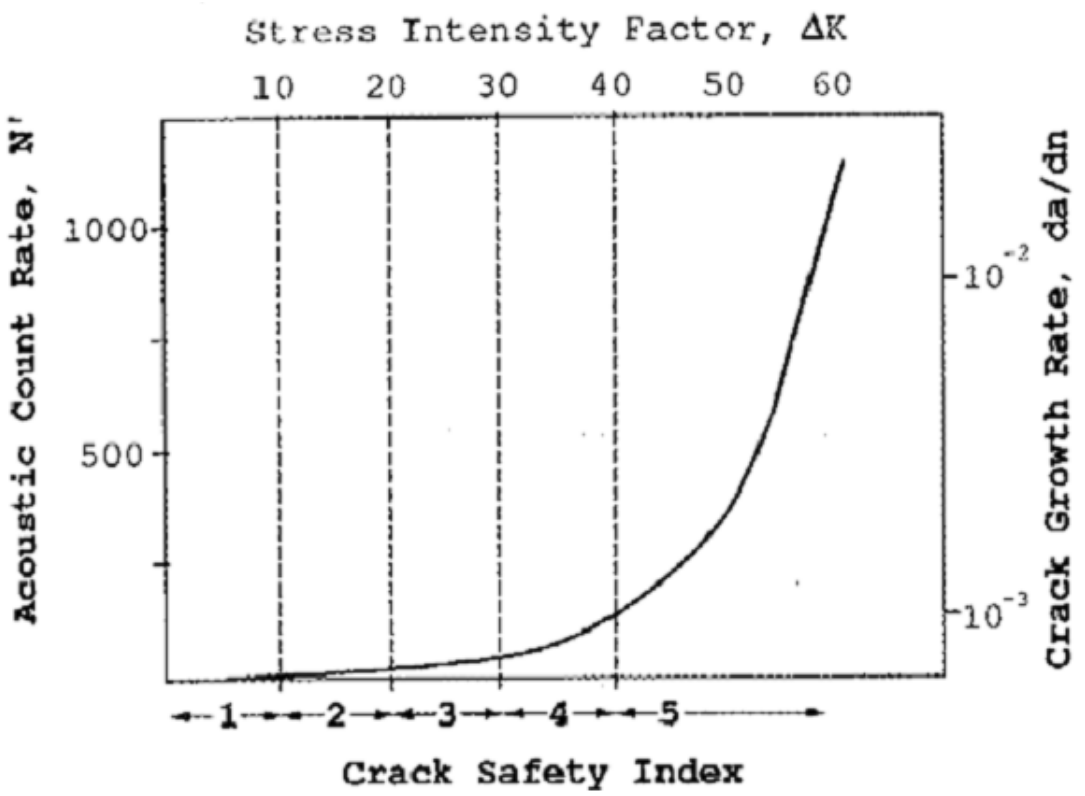

Fig. 4.2 Relationship between various parameters for classification of cracks

4.3 Historic and Severity indices

Historic and Severity index approach is also used to quantify AE data. The historic index gives a measure of the change in signal strength. The objective of historic index is to locate changes in the curve plotted against cumulative signal strength and time. The historic index is given by

$$\boldsymbol{H(I) = \frac{N}{N-K}\left(\frac{\sum_{i=K+1}^{N} S_{0i}}{\sum_{i=1}^{N} S_{0i}}\right)}$$

Severity index is another measure that uses average signal strength for specific number of events which have the largest value of signal strength. Severity index is given by

$$\boldsymbol{S_r = \frac{1}{J}\left(\sum_{m=1}^{J} S_{0m}\right)}$$

where N is the number of hits.

J and K are the material dependent constant.

and S_{0i} is the signal strength of i^{th} event.

The severity and historic index for a metal piping system is shown in figure 4.4. The regions from A to E are in the order of degree of damage.

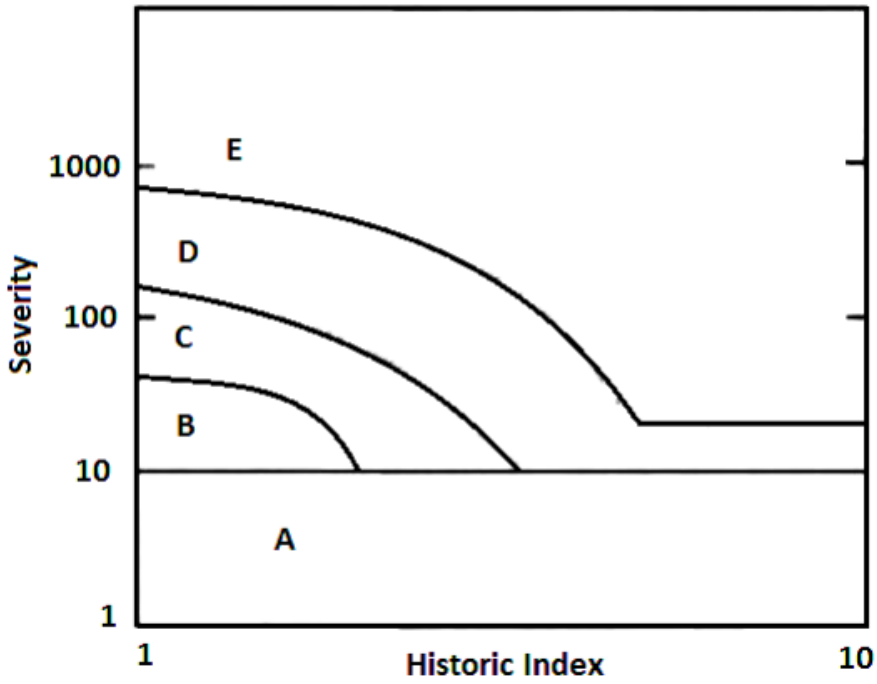

Fig. 4.4 Historic and severity index for metal piping system

4.4 *b* value analysis

It has been noticed that largely peak amplitude of AE signals is considered for assessing damage as main serious damage sources generates signals of high amplitude. These high amplitude signals before being recorded by the sensors attenuates due to scattering of signals. Thus a great care is to be taken while considering only peak amplitude for damage assessment. Hence cumulative distribution of amplitude is studied as it unambiguously changes as damage data is collected through sensors. As the damage develop the slope of cumulative distribution changes indicating increase in the ratio of large AE events to small AE events in total events collected by sensors. This technique is known as *b* value analysis. It is derived through modification of Gutenberg and Richter formula used in seismology. The Gutenberg and Richter formulae used in earthquake seismology, as a relationship between magnitude and frequency is given by

$$\mathbf{Log_{10}N = a - bM_L} \qquad \textbf{(i)}$$

Where $\mathbf{M_L}$=Richter magnitude of events or earthquake magnitudes.

N= No. of earthquakes of magnitude ≥ M.

a is the empirical constant and ***b*** is the *b* value.

In seismology this relationship quantifies the fact that earthquakes of larger magnitude occur in a small ratio than the earthquakes of smaller magnitude. M_L is proportional to logarithm of corrected maximum amplitude (data recorded in seismic trace). Attenuation in amplitude occurs as wave travel a long distance and also due to elastic absorption. A correction factor is applied to maximum amplitude (eqn. ii). The magnitude is also proportional to source rupture area (S) as

$$\mathbf{M_L\ \alpha\ (2/3)*c*Log_{10}A_{max}} \qquad \textbf{(ii)}$$

$$\mathbf{M_L\ \alpha\ (2/3)*c*Log_{10}S} \qquad \textbf{(iii)}$$

The value of **c** depends on the type of transducer used

Where c is 1, 1.5 and 3 for strain meter, velocity transducer and accelerometer.

The Gutenberg and Richter formula given by eqn. (i) is modified to be used in acoustic emission analysis. From eqn. (i) it is clear that *b* value is the negative slope of Log frequency magnitude plot. For acoustic emission analysis the modified form of eqn.(i) can be written as

$$\mathbf{Log_{10}N\ (A) = a-}\boldsymbol{b}_{\mathbf{AE}}\mathbf{*A_{dB}} \qquad \textbf{(iv)}$$

Where **N (A)** = Number of AE hits having magnitude ≥ A.

$\boldsymbol{b}_{\mathbf{AE}}$ **=** *b* value based on acoustic emission analysis.

$\mathbf{A_{dB}}$ = Amplitude in dB.

The parameter to calculate signal amplitude A is $(dB)_{AE}$ and it is given by

$$\mathbf{(dB)_{AE} = 20\ Log\ (V_p\ /\ V_{ref}\ )} \qquad \textbf{(v)}$$

Where $\mathbf{V_p}$ = Maximum signal voltage in microvolts.

AE amplitude is given by

$$\mathbf{A_{dB} = 20\ Log_{10}\ (A_{max}\ /\ A_{ref})} \qquad \textbf{(vi)}$$

Using eqn. (vi) in eqn. (iv) we get

$$\mathbf{Log_{10}N\ (M) = a\text{-}\mathit{b}_{AE} * (20\ Log_{10}A_{max})} \qquad \mathbf{(vii)}$$

Using eqn. (ii) in eqn. (i) and comparing with eqn. (vii) we get

$$\mathbf{20*\mathit{b}_{AE}*Log_{10}A_{max} = (2/3)*\mathit{b}*c*Log_{10}A_{max}}$$

Suppose a velocity transducer is used with c=1.5 then

$$\mathbf{b_{AE} = (b/20)}$$

Thus the modified form of Gutenberg and Richter formula to be used in AE analysis becomes

$$\mathbf{Log_{10}\ N(M) = a\text{-}b*(A_{dB}/20)}$$

The *b* value changes during various stages of damage evolution. It becomes high when micro cracks generates and then attain lower value when macro cracks develop thus making it a good tool to be used in characterizing stages in damage process.

4.5 Improved *b* value analysis (I*b*)

Main problem with the *b* value method is that most of time, frequency and magnitude is not strictly linear. Thus it is necessary to have a modified analysis and it is known as improved *b* value analysis. It uses statistical representatives of amplitude *i.e.* mean and standard deviation.

The improved *b* value is given by

$$\mathbf{I\mathit{b} = \frac{LogN\ (x_1)\text{-}LogN\ (x_2)}{(\alpha_1+\alpha_2)\ \sigma}}$$

and

$$\mathbf{x_1 = \mu - \alpha_1*\sigma}$$

$$\mathbf{x_2 = \mu + \alpha_2*\sigma}$$

where **μ** = Mean amplitude for the set of data under consideration.

σ = Standard deviation for the set of data under consideration.

α_1 and **α_2** are constants.

I*b* value is obtained for a set of events (50 to 100) for better results. In present study a group of 100 events with an overlap of 20 events are considered to calculate I*b* value. I*b* value for first 100 events is calculated then for 21 to 120 events and so on with an overlap of 20 events. A

code has been developed to calculate I*b* values from the AE data recorded by the sensors during testing.

4.6 Concluding remarks

The damage quantification tools used in AE are discussed. These tools helps in predicting the state of health or damage in a structure so that appropriate actions to be taken for any defect found during monitoring. In the present study I*b* value has been studied to compare and understand the failure mechanism in ductile and brittle materials.

Chapter 5

Experimental Methodology

5.1 General

The objective of this study is to investigate and compare failure mechanism in ductile material in tension, bending and in brittle material under compression with the help of acoustic emission analysis. The ductile material is subjected to varying loading conditions in tension and bending. I*b* value analysis has been carried out on the AE data recorded by sensors. The variation of I*b* is further applied to have a relationship between the failure stages and I*b* values.

5.2 Test Program

The test program involves the experimental plan is focused to evaluate both ductile and brittle media. Steel and concrete has been chosen ductile and brittle materials respectively in the present study.

For ductile materials, M.S. specimens have been used in 3-point bending as well as tension test. Size of M.S. specimen for bending and tensile tests are respectively 500 mm x 25 mm x 6 mm and 450 mm x 25 mm x 6 mm. A notch of 45˚ has been machined in tension side of M.S. specimen used in bending test so that crack under loading may initiate.

For brittle materials concrete cubes has been used. Size of concrete cubes for compression test is 150 mm x 150 mm x 150 mm. Cubes are cured for a time period of 3 and 7 days. Curing is the process of protecting concrete from loss of moisture and is kept within a permissible temperature range.

Two AE sensors are mounted on one face of M.S. specimen and on two faces of concrete cubes for the purpose of AE monitoring. A comparison is made between the I*b* value and failure mechanism in steel and cubes. I*b* value for different types of material is compared.

A flow chart showing the complete experimental procedure is as represented below.

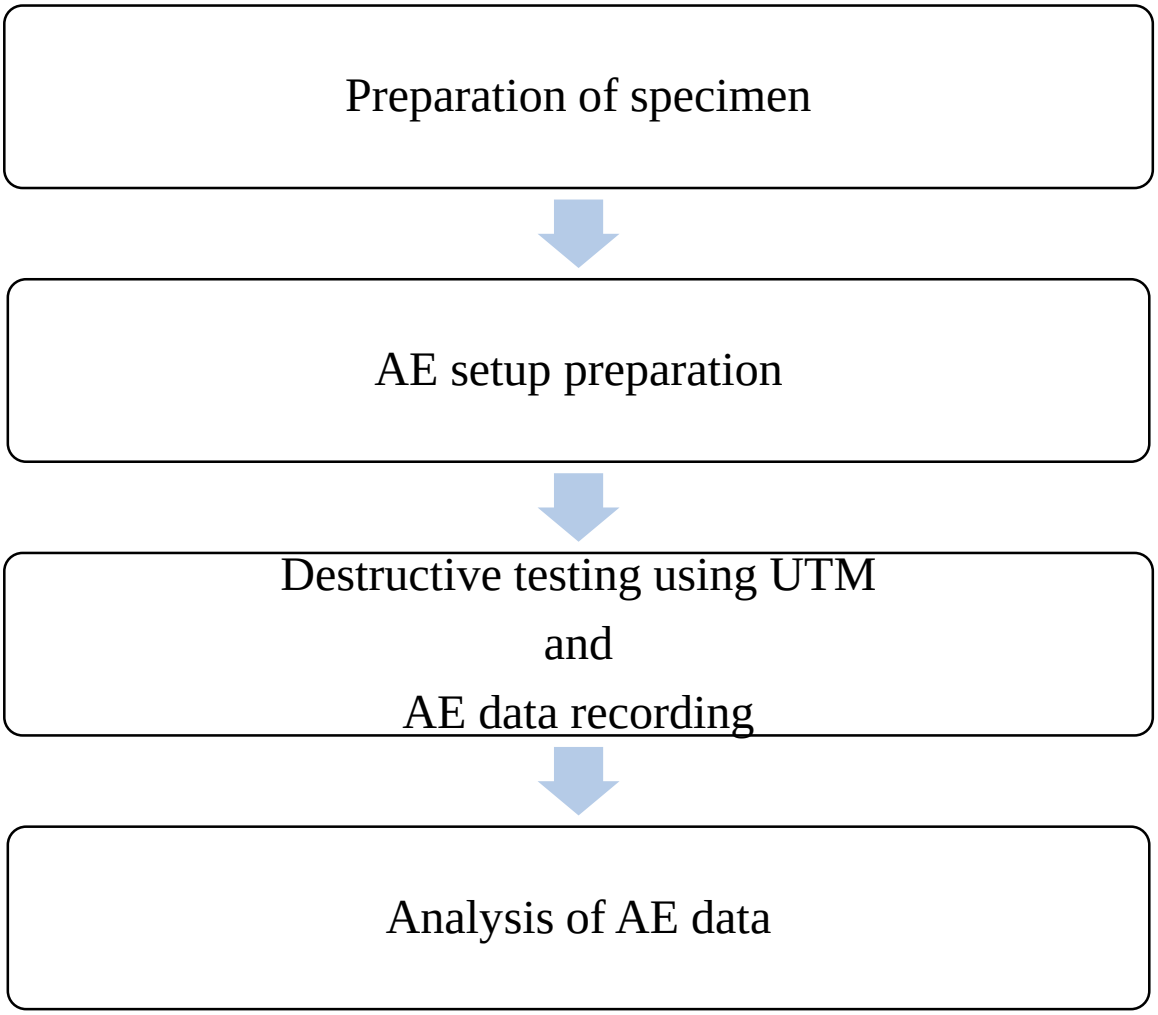

Fig. 5.1 Flow chart for test program

Experimental procedure as laid out earlier has been explaimed.

5.3 Materials Used

Different types of materials are used in the formation of ductile and brittle specimen and they are as follows

5.3.1 Mild Steel

M.S. is a common and most widely used engineering material. It is also known as plain carbon steel. It is used in various applications due to following reasons:-

- It is cheaper.
- It provides properties that are acceptable to many applications.

It contains 0.05 to 0.15 % carbon. Due to low percentage of carbon it is more malleable and ductile. It has low tensile strength. To increase its surface hardness carburizing is performed. The mild steel has a density of 7861.093 Kg/m$^{5.}$ It has a young's modulus of 210 GPa. A moderate amount of carbon make mild steel different from other steel. In the interstitial sites of iron lattice carbon atoms get affixed thus making mild steel stronger and harder but its increased hardness comes at the cost of decrease in ductility. It is much ideal for welding purpose as without defiling metal surfaces it conducts current effectively. As compared to other grades of steel which are brittle, mild steel is hard but it is malleable thus making it an important material for making pipelines, cookware and other construction materials.

5.3.2 Cement

Portland Pozzolana Cement (PPC) is used to cast cubes to be tested as brittle material. It is a type of cement produced either by intergrinding of gypsum with OPC clinker and pozzolanic materials in defined proportions or grinding OPC clinker, gypsum and other pozzolanic materials separately and then blinding them thoroughly in defined proportions. Ambuja Cement PPC has been used in this study to cast cubes.

Key properties of PPC cement are listed as under

- The cement particles in PPC have spherical shape and have higher fineness value. The spherical shape allow concrete to move freely. The higher fineness value allows better filling of pores.
- For a given workability it decreases bleeding (casting become porous and weak) by providing greater fines volume and low water content.
- It gives better finishing.
- The compressive strength is large than OPC at later ages.
- Due to slower hydration it generates lower internal stresses.
- Shrinkage is lower in case of PPC.

5.3.3 Other materials

Sand aggregates and water were also used in making cubes.

5.4 Preparation of Test Specimens

5.4.1 Mild Steel Specimens

Mild steel specimens of dimension 500 mm x 25 mm x 6 mm and 450 mm x 25 mm x 6 mm were prepared to carry out experiment on ductile materials. Steel specimens were loaded in tension and bending. Two specimens have been used to test the repeatability of tests. In tensile and bending varying loading conditions have been used. In tensile testing, loading has been done with varying strain rates. Similarly in bending test, varying load rates have been used. Table 5.1 and 5.2 show the test methods for tensile and bending tests carried out on UTM.

Table 5.1 Mild steel plates loading description in tension

Type of loading	Strain rate
Tensile Loading	10 mm/min
	20 mm/min
	30 mm/min

Table 5.2: Mild steel plates loading description in bending

Type of loading	Loading rate
Bending	20 kN/min
	30 kN/min
	40 kN/min

5.4.2 Concrete Cubes

M25 concrete cubes of dimension 150 mm x 150 mm x150 mm are casted with the help of Ambuja PPC cement, sand, aggregates and water. Cement, sand and aggregates are mixed in the ratio of 1:2:4. For M25 concrete cubes following procedure is adopted to get the final amount of cement, sand and aggregates.

Let X be the amount of cement required to cast one cube. Then 2X and 4X is the required amount of sand and aggregates respectively. The sum of quantities of cement, sand and aggregates are then made equal to the product of volume of cube. Then the quantity of cement

and after that the quantity of sand and aggregates is calculated. The ratio of water to cement is taken as 0.45. Figure 5.2 shows the casing used for casting cubes.

Fig. 5.2 Casing used for casting concrete cubes

Cement, sand, water and aggregates are then properly mixed and the mixture is poured in casing to take the shape of cube. A vibrating table is also used for setting mixture in casing so that no voids remain in the concrete cube. Figure 5.3 shows the vibrating table used in casting concrete cubes.

Fig. 5.3 Vibrating table used for setting concrete

The cubes are then taken out of casings after 24 hours and kept in water for curing. The time period for curing is taken as 3 days and 7 days. The curing is done to protect concrete from losing moisture.

5.5 Acoustic Emission Monitoring

Acoustic emission setup was installed to monitor fracture mechanism. The equipment discussed below were used to capture AE data. Threshold was set at 40 dB after performing pencil lead break test. The preamplifier gain was set at 40 dB.

5.5.1 Setup details

- **Micro-II Digital AE system**

  AE data acquisition system used in the present study is Micro II digital AE system provided by PAC (Physical Acoustics Corporation) **MISTRAS GROUP** shown in Fig. 5.5.

Fig. 5.5 Micro-II digital AE system

It holds up to 32 AE channels. It is directly connected to monitor. It includes a low power CPU, USB ports and integrated LEDs which give indication of AE hits.

- **Sensors**

  Sensors are mounted on the surfaces of specimens. Two different types of sensors are used in the present study. One type of sensor is used in the monitoring of ductile material (mild steel plates) and other is used in the monitoring of brittle materials (concrete cubes).

The two types of sensors used are as

(a) R15α sensor

This is a general purpose sensor having high intensity and low frequency rejection. It is used in various applications like vessels, pipelines, bridges, chemical plants as well as in applications related to factory and process monitoring. Figure 5.6 shows R15α sensor used in present study.

Fig. 5.6 R15α sensor

Table 5.3 depicted below has the specifications related to R15α sensor.

Table 5.3 Specifications of R15α sensor

S.No	Specification	Value
1	Dimension	0.75” dia. x 0.88” h
2	Weight	34 gm
3	Case Material	Stainless Steel
4	Face Material	Ceramic
5	Operating frequency range	50 – 400 kHz

(b) R3α sensor

This is a general purpose sensor and boasts low frequency, 30 kHz resonant response. Thus it is useful in tight areas which require low frequency sensor for testing. This sensor is used in structural health monitoring of small concrete structures, metal pipeline leak detection and in areas where there is a need of high noise rejection. Figure 5.7 shows R3α sensor used in present study.

Fig. 5.7 R3α sensor used in present study

Table 5.4 depicted below gives the specification of R3αsensor.

Table 5.4 Specification of R3α sensor

S.No	Specification	Value
1	Dimension	0.75” dia. x 0.88” h
2	Weight	41 gm
3	Case Material	Stainless Steel
4	Face Material	Ceramic
5	Operating frequency range	25-70 kHz

- **Preamplifiers**

  It prepares an electronic signal for further amplification. 2/4/6 type preamplifier is used in this study. It has an option of 20/40/60 dB gain. It operates with either single ended or differential sensor. Figure 5.8 shows preamplifier used in present study.

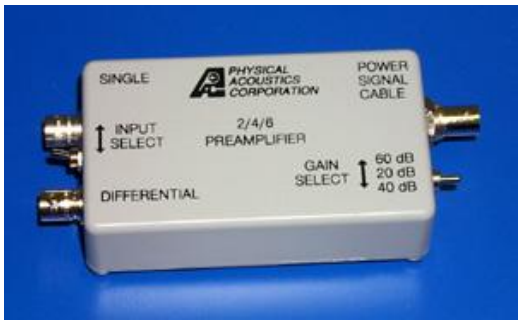

Fig. 5.8 Preamplifier used in the study

Following are the features of 2/4/6 preamplifier

- 20/40/60 selectable gain.
- Low noise.
- Plug in filters
- Input Protection.

5.6 Universal Testing Machine (UTM)

UTM is used to test the compressive and tensile strength of material. It is named so because it can perform various standard tensile and compressive test on materials. In present study Hung Ta Instrument Co., ltd UTM is used. It has a capacity of 1000 kN. All loading conditions (tension, bending and compression) are applied with this UTM. The loading conditions can be set by two ways. One is to enter the input in the panel provided along with the machine and second method is to enter the values in UTM program provided by the manufacturer. The

machine can be operated with the help of UTM program. There is a procedure to be followed to operate machine with the help of UTM program. The procedure is as follows

- Specify specimen in the specimen editor and loading condition in the method editor
- Make test program number in new instruction section and run test.

The UTM machine used in present study is shown in Fig. 5.9.

Fig. 5.9 UTM machine used in study

The system for running UTM with the help of computer program is shown in Fig. 5.10.

Fig. 5.10 Setup used to operate UTM with computer

Running UTM with UTM program helps in giving various plots which can be analysed to get useful information. Plots like load-displacement, stress-strain, load-time etc. are obtained. Figure 5.11 shows one of load-time graph obtained in experiments carried out in the study.

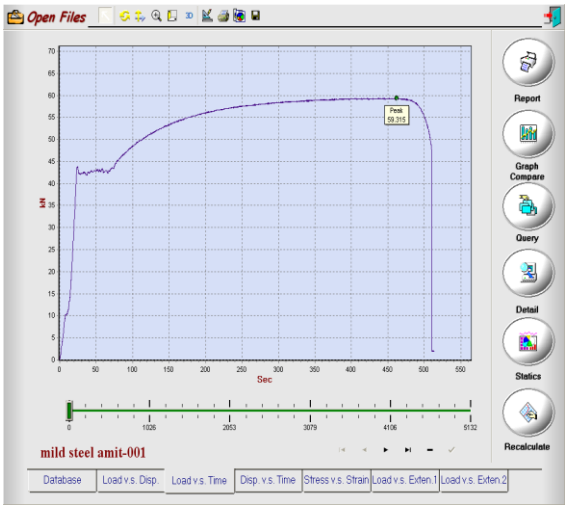

Fig. 5.11 Load-Time Variation

It also gives a text file containing load, time and extension values generated in the experiment. So another way of getting these plots is to manipulate the data generated by the machine. The sensors are mounted on the plates at a distance of 120 mm in tensile loading and at 150 mm in bending and compression. The experiments are carried out at various loading rates and the data generated by AE setup is analysed. I*b* value is calculated for each loading condition with the help of MATLAB program. I*b* value calculated are then analysed to have useful information about the fracture mechanism.

5.7 Process flow to calculate I*b* value

I*b* value was calculated using the methodology explained in the flowchart. The I*b* value was calculated for 100 events with an overlap of 20 events i.e. I*b* value for 1 to 100 events was calculated then I*b* value for 21 to 120 events was calculated and so on. The methodology adopted to calculate I*b* value for 100 events for sensor 1 out of complete AE data is shown in Fig. 5.12.

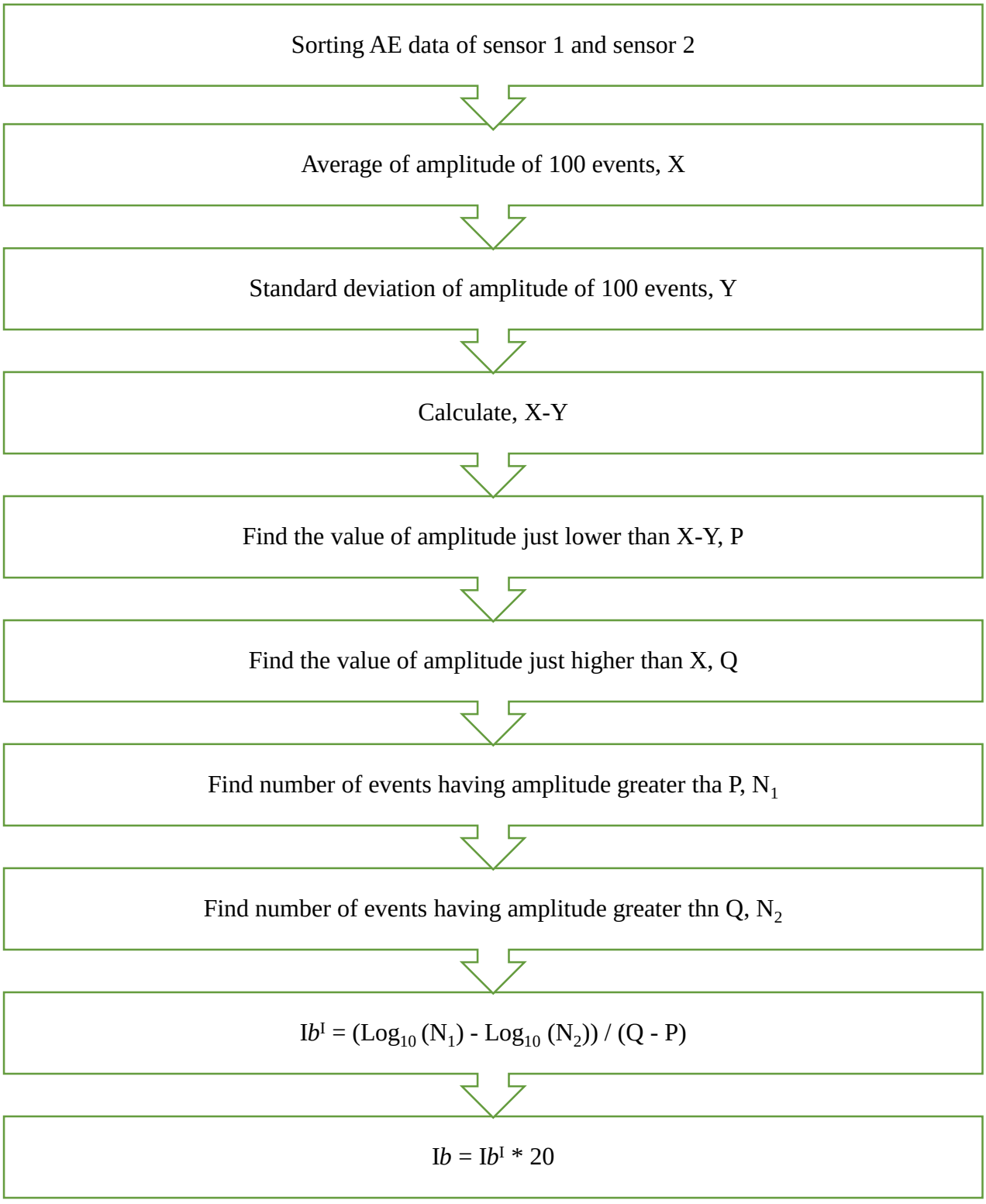

Fig. 5.12 Flow process to calculate I*b* value.

Chapter 6

Results and Discussions

6.1 Introduction

The previous chapter focused on the conditions and parameters to carry out the experimentation work. Experiments were performed on both ductile and brittle material. According to the conditions required for experimentation, the required equipment were selected. This chapter focuses on the experimentation carried out and the results obtained from the experiment. Acoustic emission testing was performed and obtained data was analysed to obtain improved *b* value for both ductile and brittle material.

6.2 Results from Tensile Loading for ductile materials

The M.S specimens of dimension 450 mm x 25 mm x 6 mm were loaded in tension at various strain rates as discussed in the previous chapter. The data obtained from acoustic setup was compared with UTM data to study fracture mechanism in mild steel and to study the behavior of acoustic emission parameters like amplitude, absolute energy etc. during fracture mechanism. The results obtained in tension are discussed below.

6.2.1 Tensile test of Steel specimen at 10 mm/min rate of loading

The loading rate of 10 mm/ min was applied to two mild steel specimens to ensure repeatibilty of acoustic emission data analysis and the results were obtained from both UTM program and acoustic emission setup. The load versus time plot obtained from UTM program for first specimen is shown in Fig. 6.1. The amplitude versus time plot for the loading rate of 10 mm/min is shown in Fig. 6.2. The I*b* versus time plot obtained from I*b* value analysis is shown in Fig. 6.3.

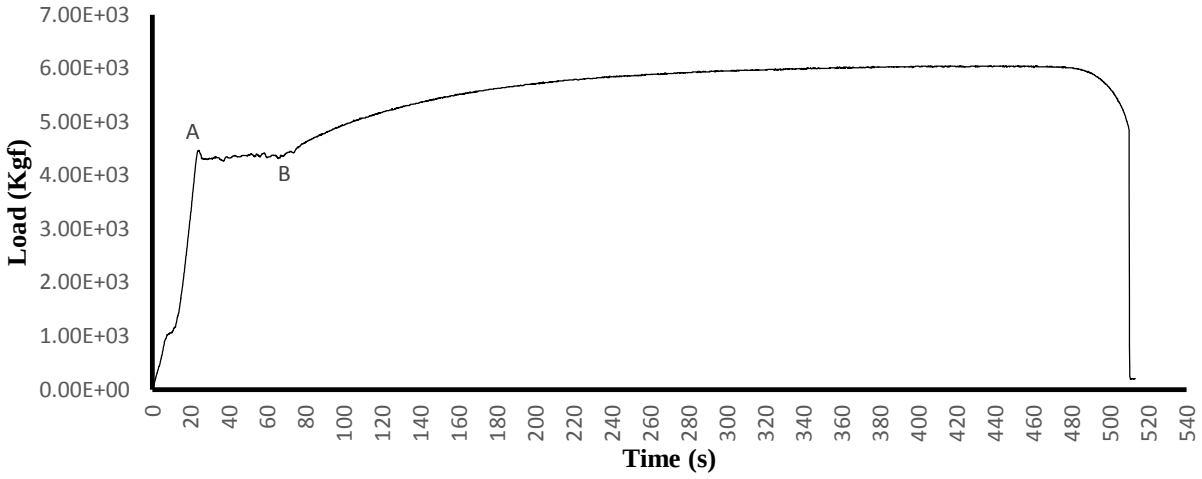

Figure 6.1 Load vs time for 1st specimen.

In Fig. 6.1 O-A represents the linear elastic limit. Up to the elastic limit i.e. point A the applied load is directly proportional to the displacement produced in the material. Beyond point A permanent deformation of material occurs. Region A-B contributes toward permanent deformation of mild steel specimen. Beyond point B load increased to a peak value followed by necking and ultimate failure of material. The amplitude and absolute energy are plotted against time and shown in Fig. 6.2 and 6.3.

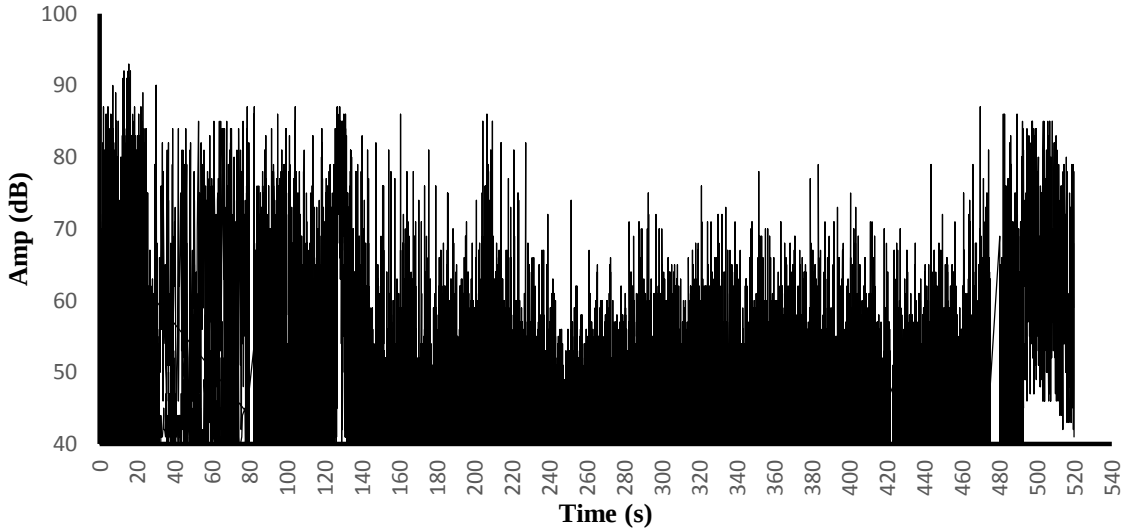

Figure 6.2 Amplitude vs time for 1st specimen

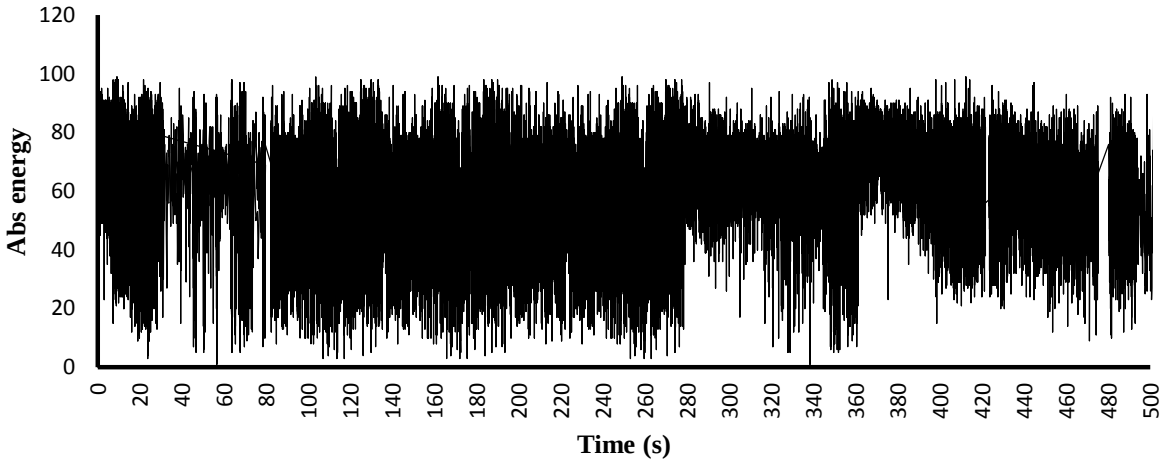

Figure 6.3 Absolute energy vs time for 1st specimen

In the linear elastic limit up to point A, normal AE activity occurs. Initial adjustments in the UTM setup also contributes to the recorded AE activity. When the load increase beyond region OA, yielding phase begins to appear. In this transformational phase, there are lot of AE events with substantial amplitude and energy observed. This may be primarily attributed to the movement and amalgamation of microcracks, voids and defects related to crystal lattice which are inherently present in the material. However during this phase, no visible crack growth and propagation was observed in the specimen.

Beyond point B, load continuously increases and permanent deformation sets in. AE events with substantial amplitude been recorded during this phase. However amplitudes are not as large as in the earlier phase (A-B). When the load approaches its maximum value then necking was observed on the specimen and spurt of AE activities was also recorded. Beyond this stage load suddenly falls paving way for rapid crack growth. Hence from the AE experimental data it can be observed that maximum AE activity is recorded during the transformation of elastic to plastic region. This is the phase when the yielding is set to start resulting in the localization of various microvoids and inherent defects (like crystal dislocations, microinclusions etc.) to merge, giving rise to crack front and its subsequent propagation. However high amplitude and energy events recorded during the transformational yielding phase (A-B), no visible damage/crack could be observed with naked eyes. The *b* value analysis was applied to the data captured by AE setup and is shown in Fig. 6.4.

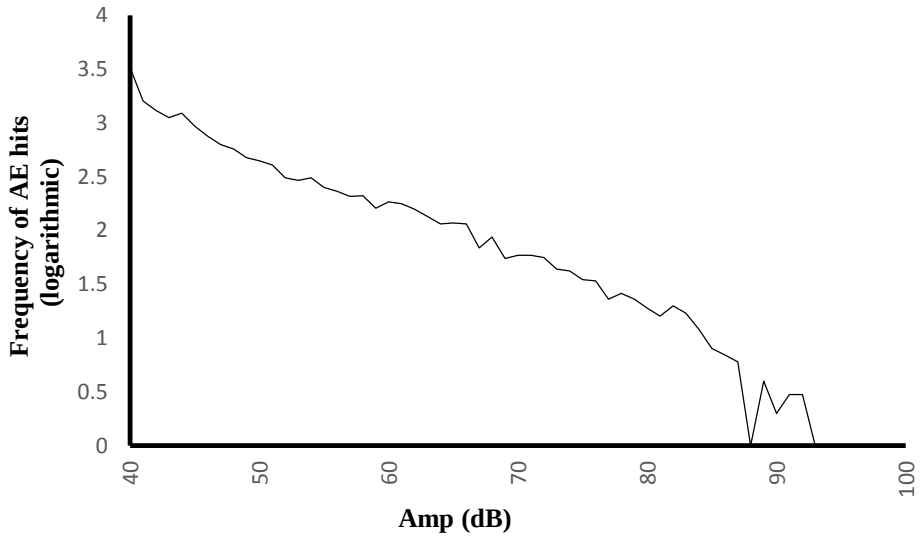

Figure 6.4 Log frequency magnitude plot for 1st specimen

The *b* value analysis was applied to the captured data and a nonlinear relationship between frequency and magnitude was found. The *b* value is the non-negative slope of the log frequency magnitude curve. Thus improved *b* value analysis was applied on the captured data. The I*b* for the initial regions is plotted against time and is shown in Fig. 6.5.

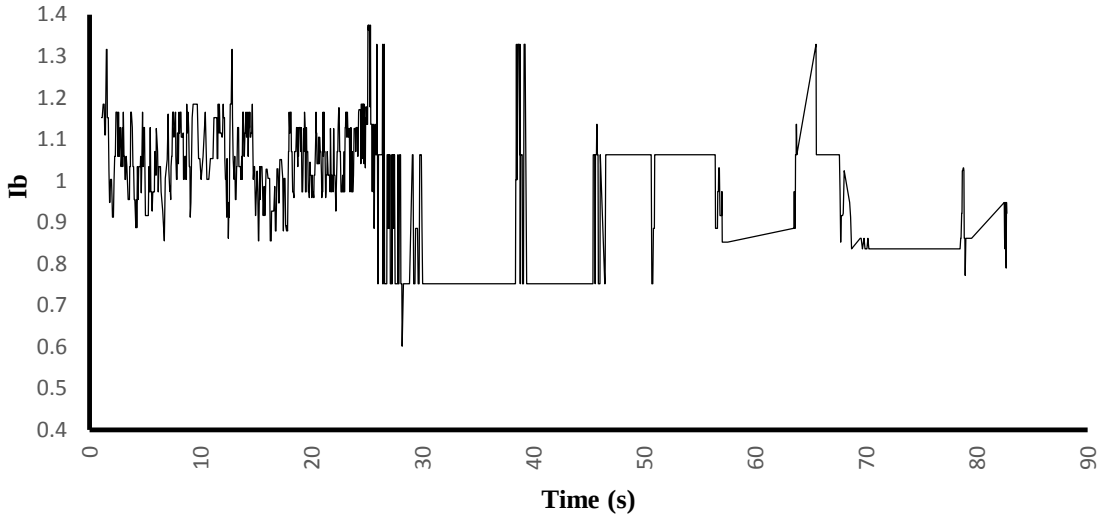

Figure 6.5 I*b* value vs time for first specimen

I*b* value plotted against time was then studied and it had been observed that the lower I*b* value equal to 0.60 was found in the transformational elastic to plastic region. AE data for second specimen was then analysed to ensure repeatability of the method used in present study. The variation of parameters discussed above were plotted against time and are shown below.

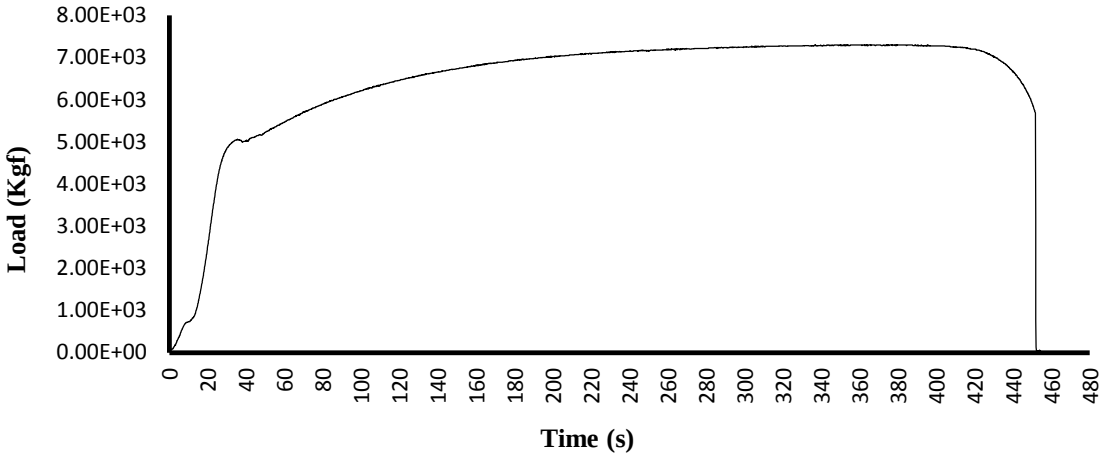

Figure 6.6 Load vs time for 2nd specimen

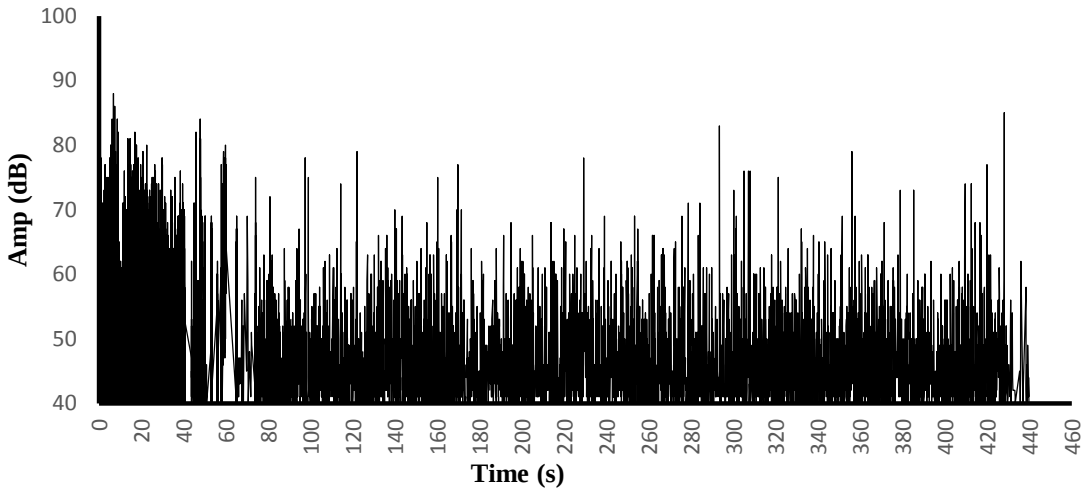

Figure 6.7 Amplitude vs time for 2nd specimen

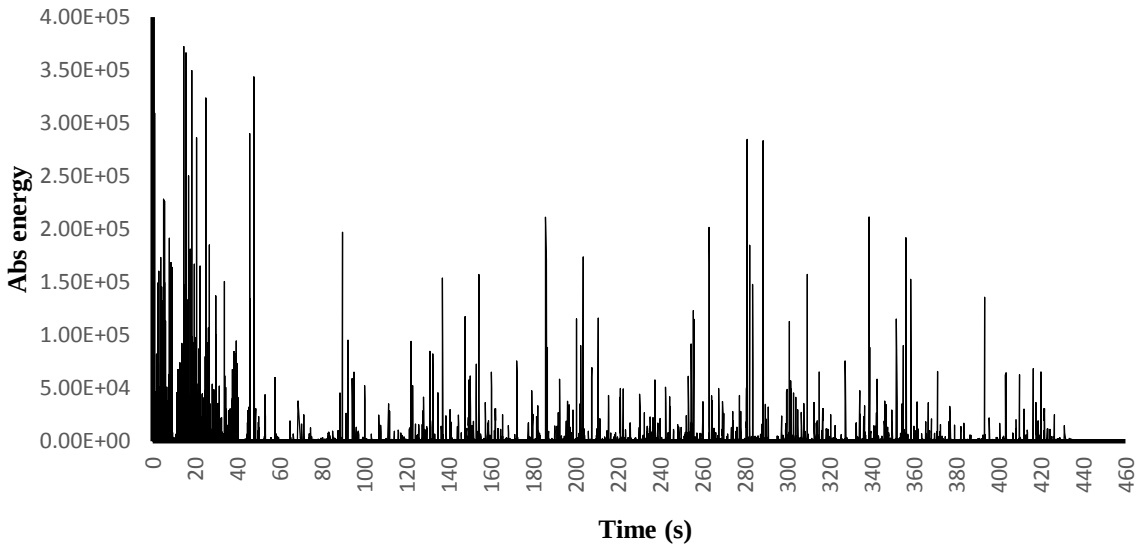

Figure 6.8 Absolute energy vs time for 2nd specimen.

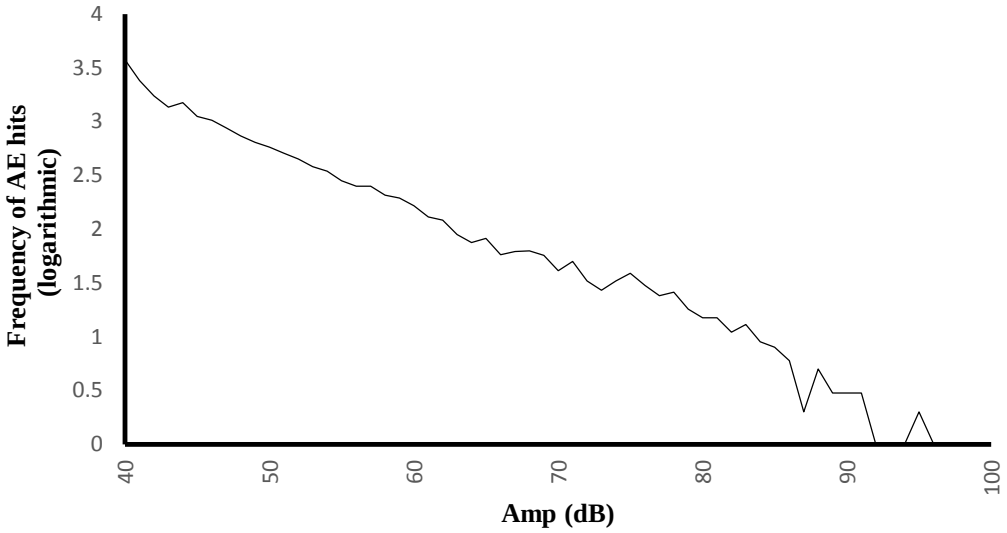

Figure 6.9 Log frequency magnitude plot for 2nd specimen

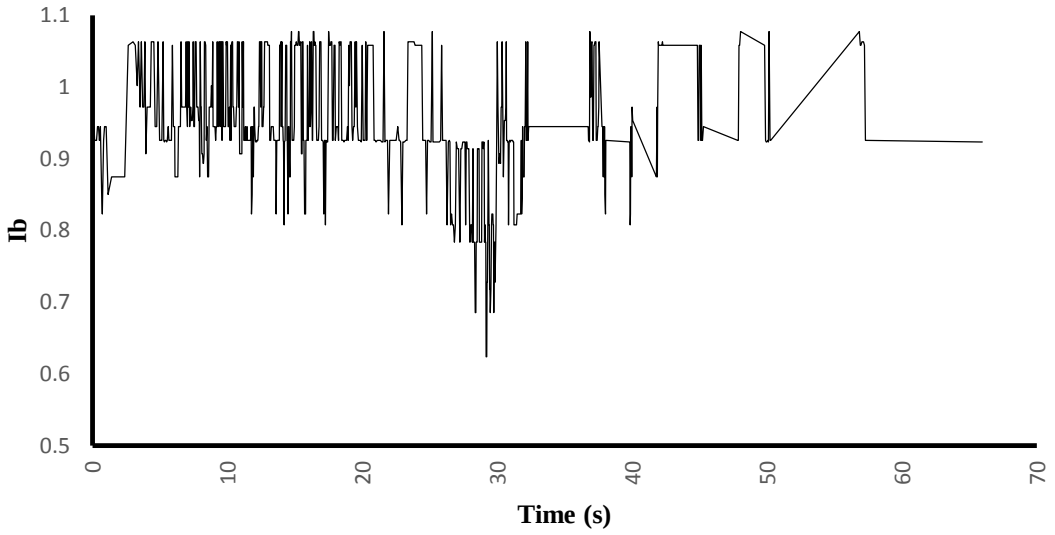

Figure 6.10 Ib value vs time for 2nd specimen

The lower I*b* value in the transformational yielding region was found equal to 0.62 for second specimen loaded at the strain rate of 10 mm/min. Similar observations were made for strain rates of 20 mm/min and 30 mm/min and related experimental results are discussed below.

6.2.2 Tensile test of Steel specimen at 20 mm/min rate of loading

The loading rate was then increased to 20 mm/min and AE parameters discussed above were plotted against time to study fracture mechanism at 20 mm/min rate of loading. The AE parameters along I*b* value were plotted against time.

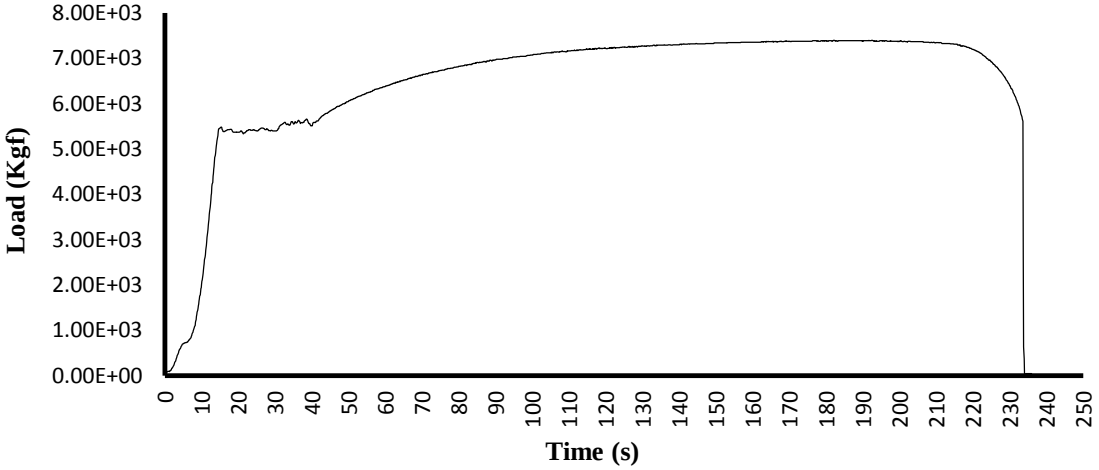

Figure 6.11 Load vs time at 20 mm/min rate of loading

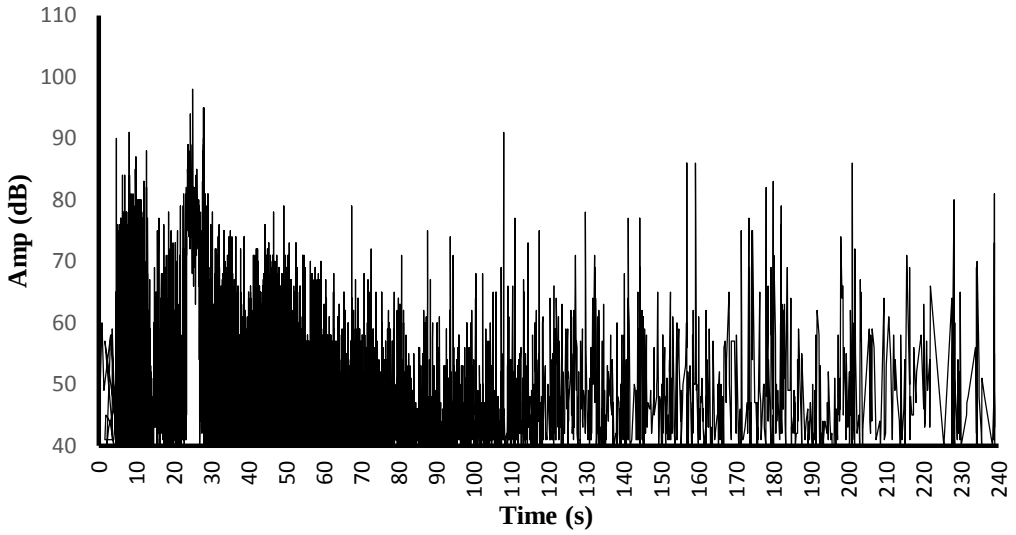

Figure 6.12 Amplitude vs time

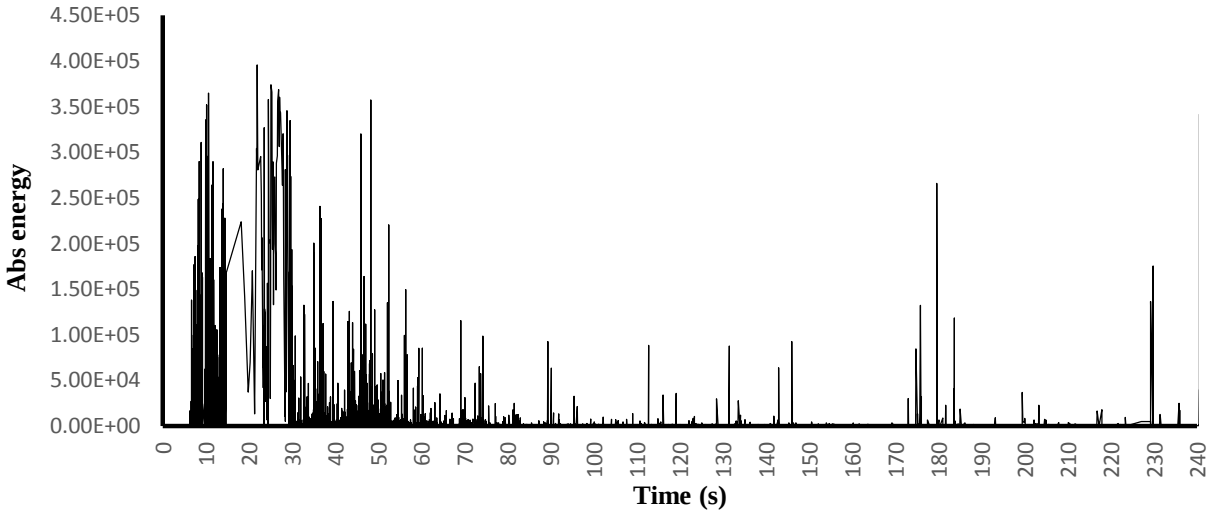

Figure 6.13 Absolute energy vs time graph

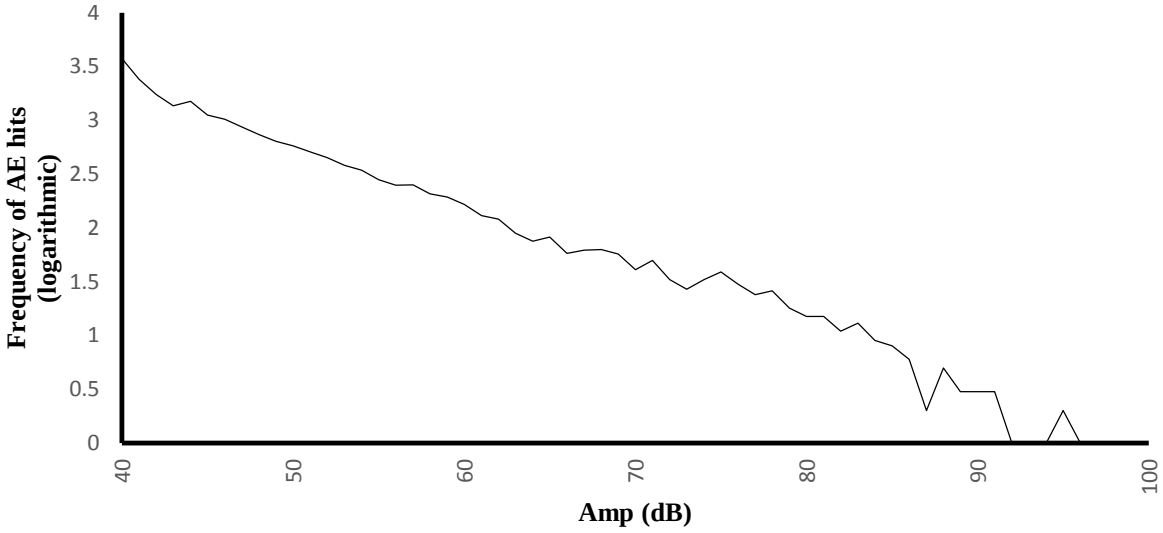

Figure 6.14 Log frequency magnitude plot

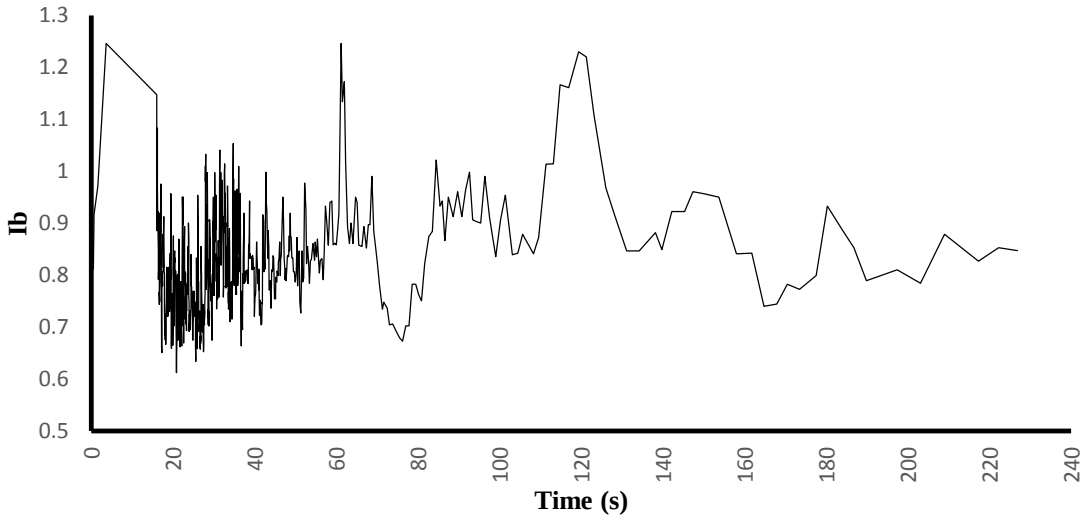

Figure 6.15 I*b* value vs time

The lower I*b* value was found equal to 0.61 at the loading rate of 20mm/min in the transformational yielding phase. The lower I*b* value was found prior to the case of 10 mm/min. It justifies that I*b* value decrease with the increase in loading rate. The M.S. specimens were then tested in tensile loading at the rate of 20 mm/min.

6.2.3 Tensile test of Steel specimen at 30 mm/min rate of loading

The strain rate was then increased to 30 mm/min to observe the variation of I*b* value with increased loading rates. AE parameters along with I*b* value was plotted against time and are shown as under

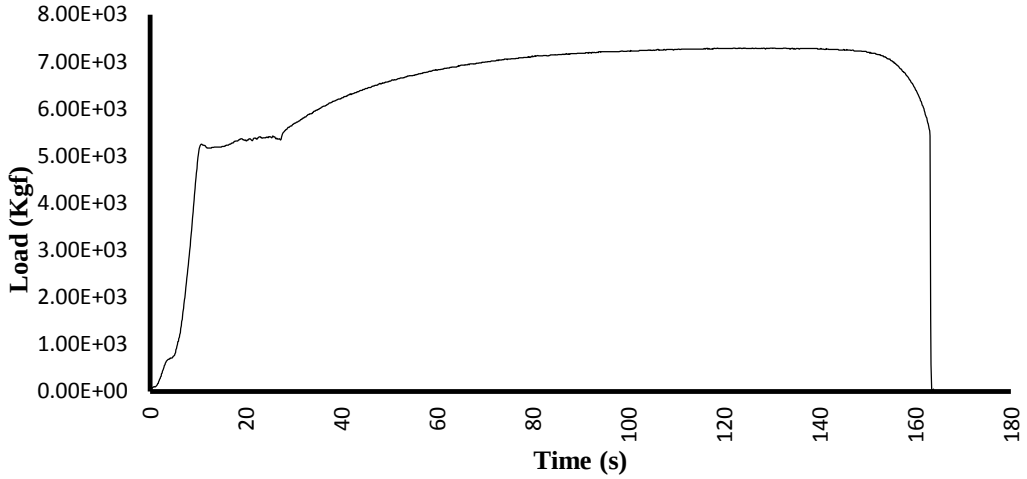

Figure 6.16 Load vs time at 30 mm/min

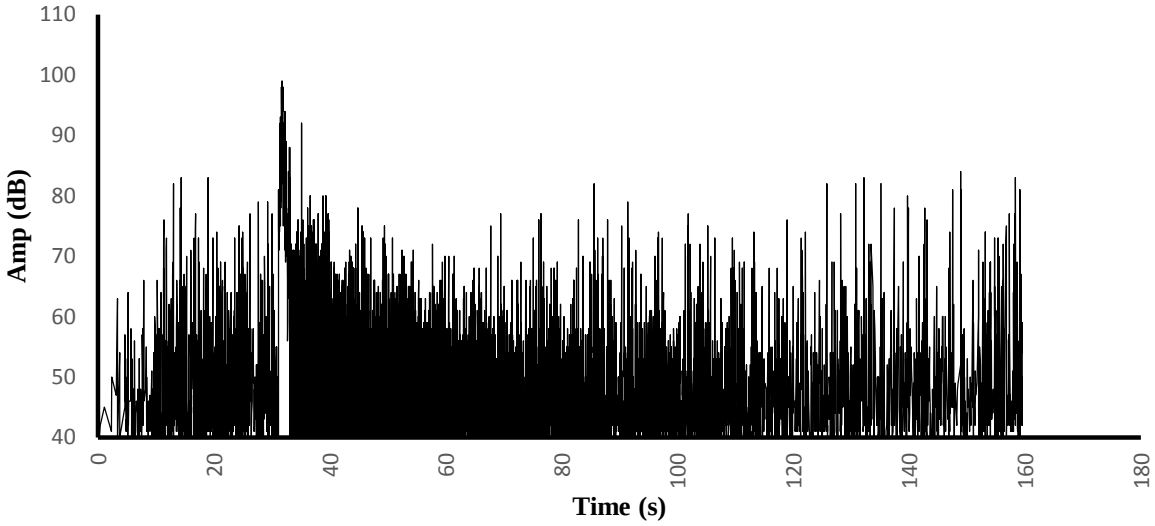

Figure 6.17 Amplitude vs time at 30 mm/min

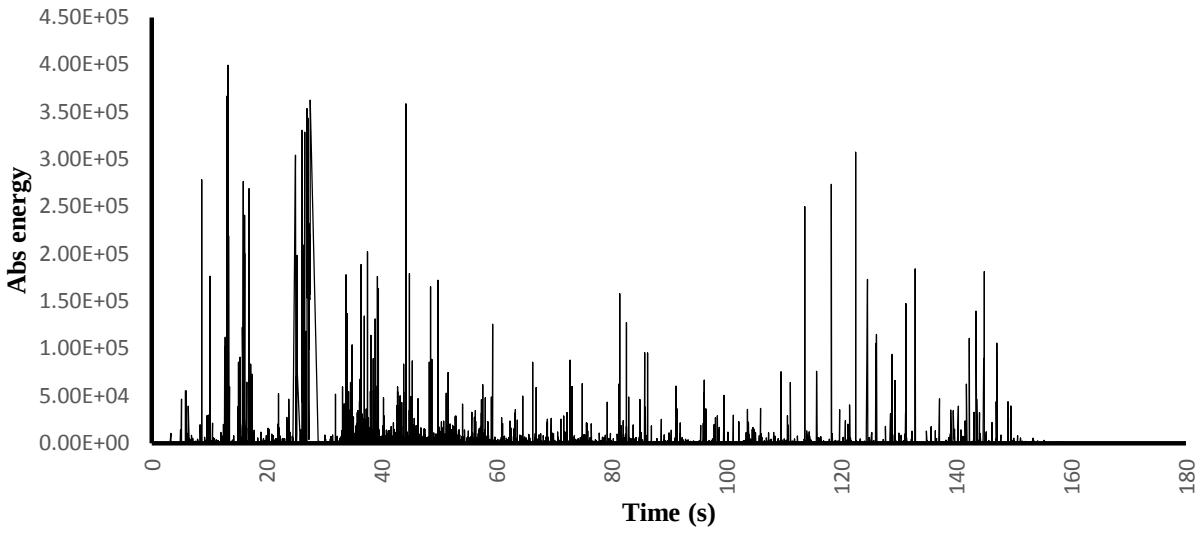

Figure 6.18 Absolute energy vs time at 30mm/min

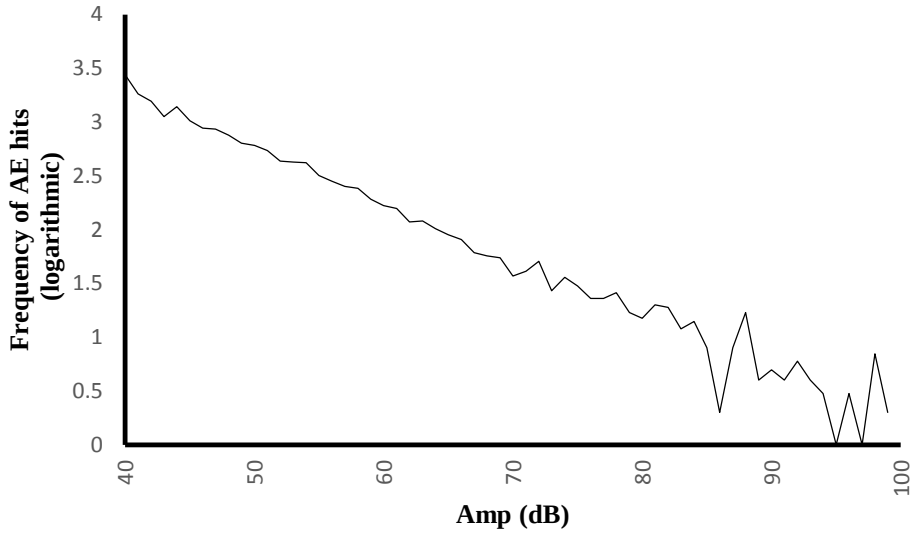

Figure 6.19 Log frequency magnitude plot at 30 mm/min

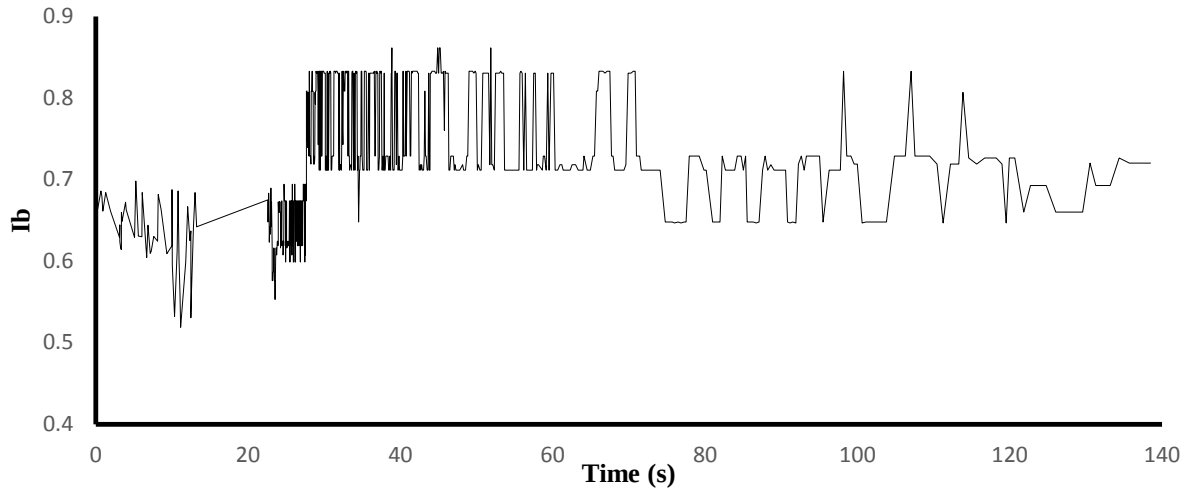

Figure 6.20 I*b* value vs time at 30 mm/min.

The lower I*b* value was found equal to 0.51 for 30 mm/min loading rate. In terms of appearance, the lower I*b* value appeared prior to lower I*b* values in 10 and 20 mm/min.

6.3 Results from Three Point Bend test

The specimens of dimension 500 mm x 25 mm x 6mm were tested for three point bend test at various loading rates. Three point bend test was carried out by applying load on the plain side setting notch on the tension side. AE parameters were plotted against time to understand failure mechanism in three point bending. The loading rate as discussed in the previous chapter was applied.

6.3.1 Three Point Bend test at 20 kN/min rate of loading

The load in three point bend test was applied with the use of UTM. The variation of AE parameters and I*b* value with time for the loading rate of 20 kN/min is shown below.

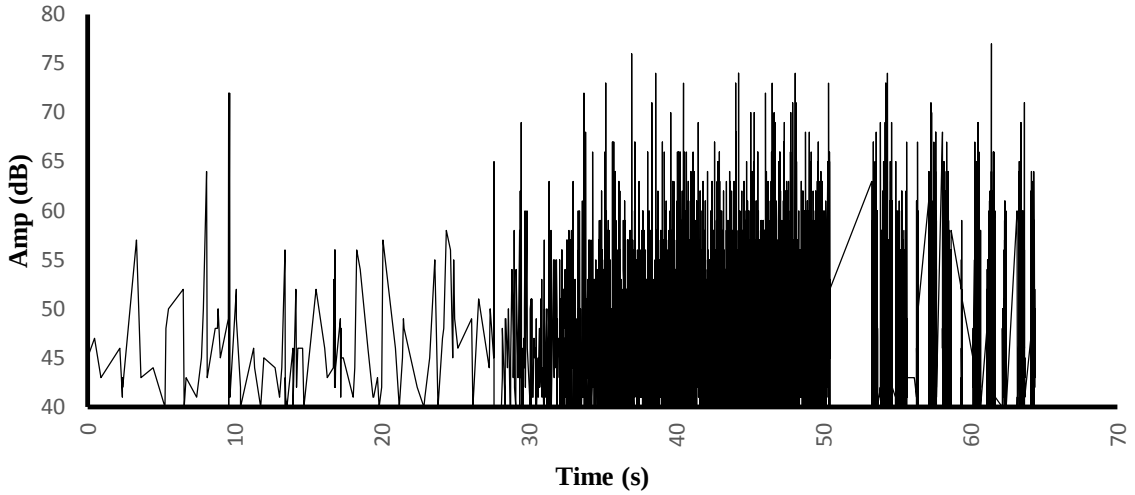

Figure 6.21 Amplitude vs time at 20 kN/min

Initially, when the load was applied, low AE activity was observed. As the load increased with time, deformation starts to occur spurting high acoustic emissions. Transformational change from elastic to plastic deformation causes high AE activity. The maximum number of events with high absolute energies also were found in this region. The variation of absolute energy with time is shown in Fig. 6.21.

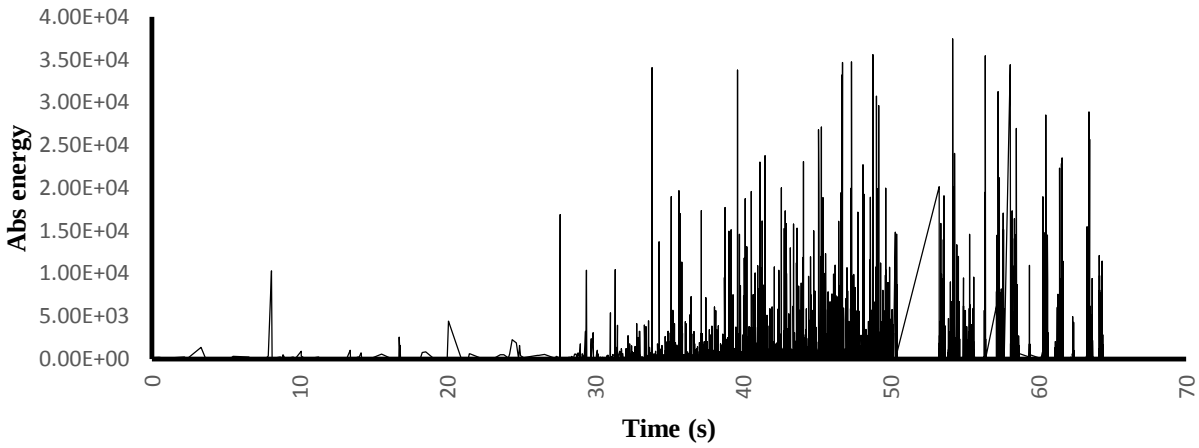

Figure 6.22 Absolute energy vs time at 20 kN/min

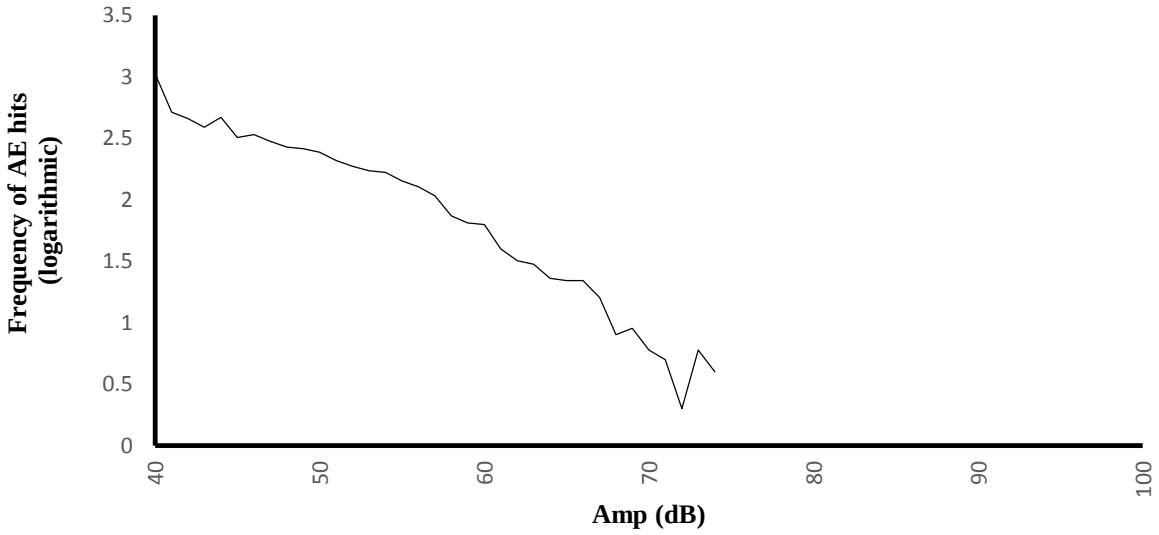

Figure 6.23 Log frequency magnitude plot at 20 kN/min

Logarithmic frequency magnitude curve was found nonlinear and improved *b* value was applied to the AE data and was plotted against time as

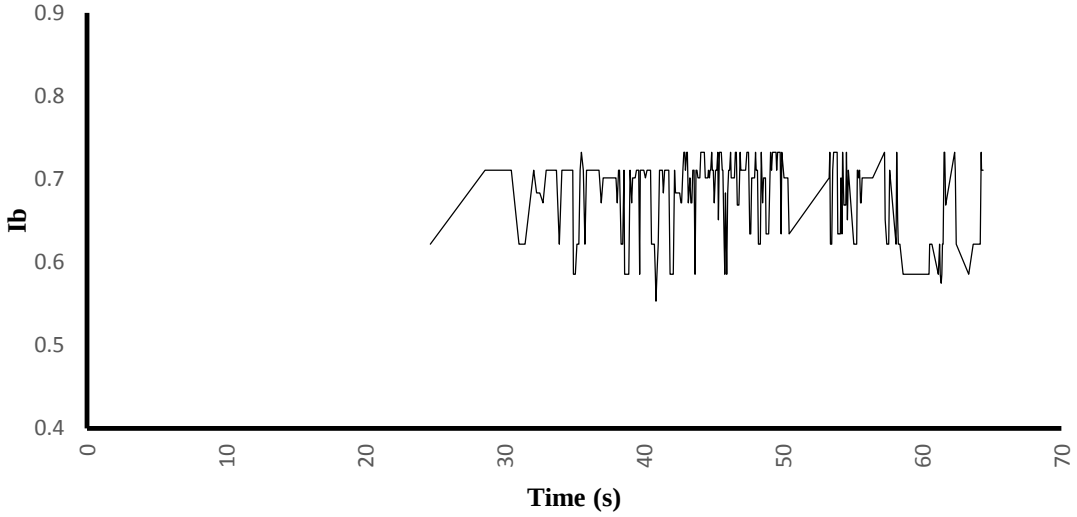

Figure 6.24 I*b* value vs time at 20 kN/min

The lower I*b* value was found equal to 0.55 for the loading rate of 20 kN/min in three point bend test. The load was then increased to 30 kN/min and AE parameters were studied with respect to time to understand fracture mechanism.

6.3.2 Three Point Bend test at 30 kN/min rate of loading

The procedure as explained in the previous section was adopted and the loading was increased to 30 kN/min. The AE parameters along with I*b* value variation with respect to time were studied.

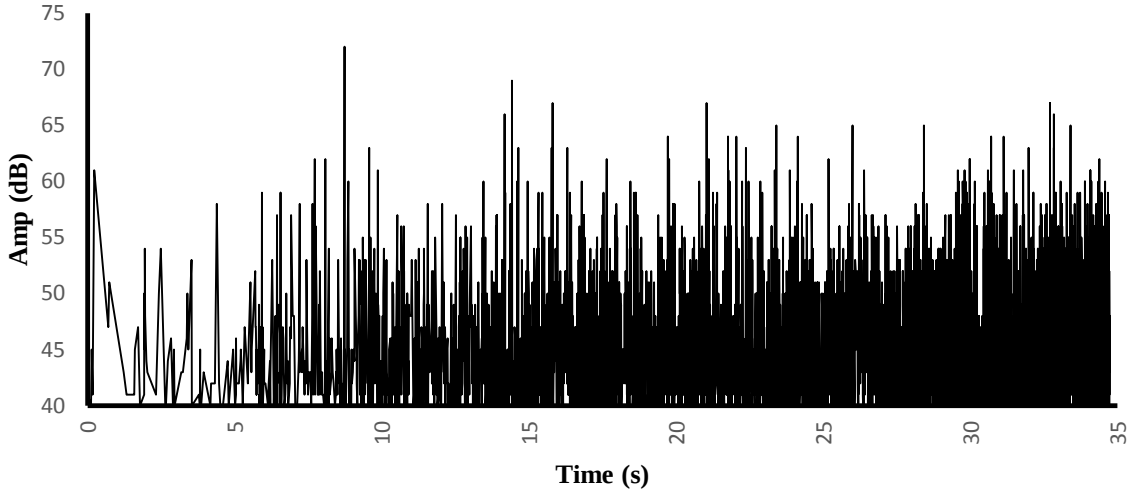

Figure 6.25 Amplitude vs time at 30 kN/min

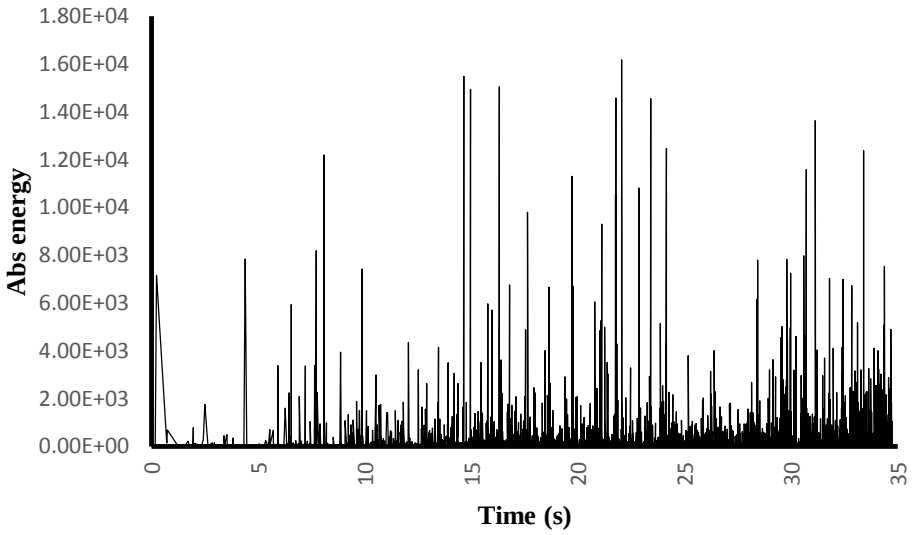

Figure 6.26 Absolute energy vs time at 30 kN/min

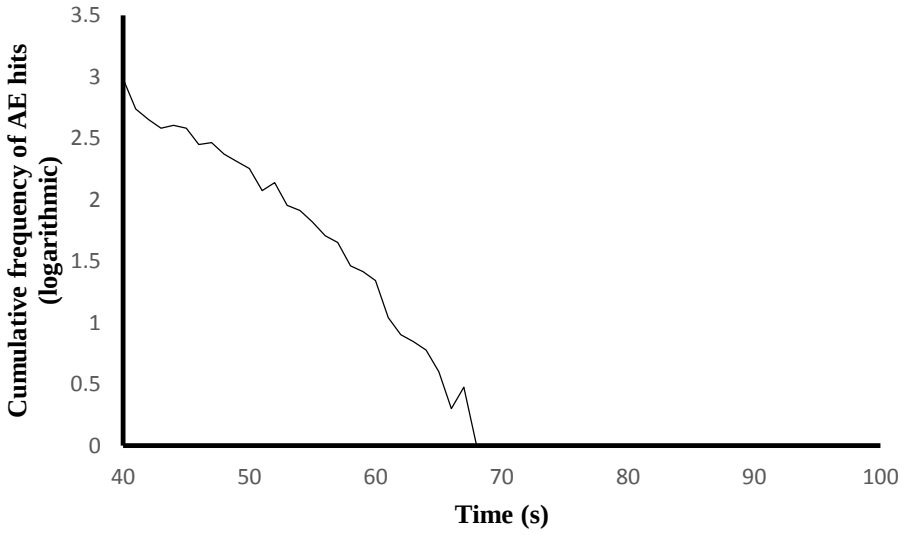

Figure 6.27 Log frequency magnitude plot at 30 kN/min

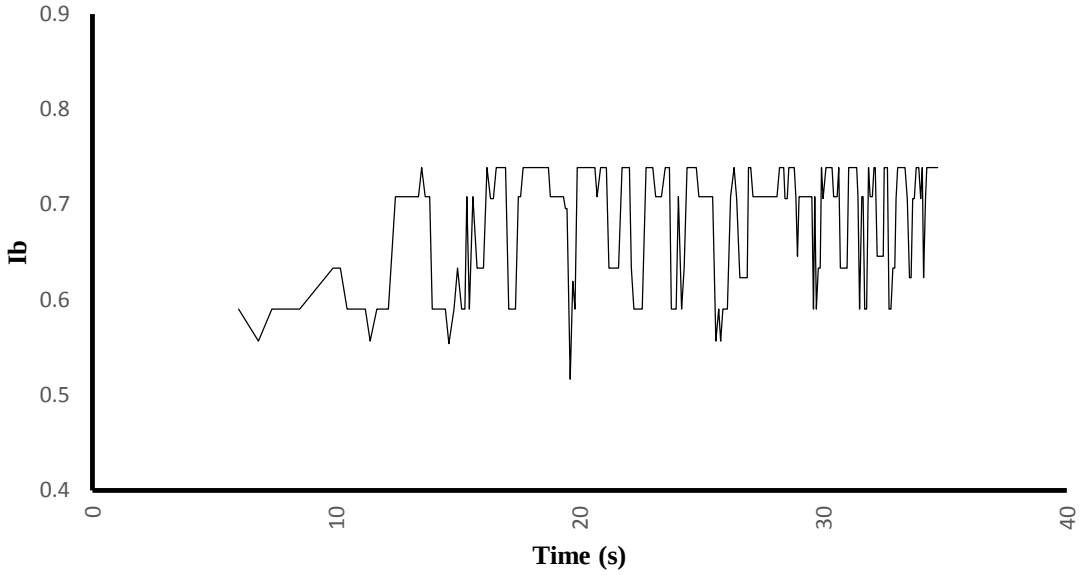

Figure 6.28 I*b* vs time at 30 kN/min

The lower I*b* value was found equal to 0.51 in the high AE activity area. Fracture mechanism for brittle material was then studied.

6.4 Results from brittle materials

The concrete cubes were tested in compression to study effect of curing and effect of variable loading on the brittle materials. The cubes cured in water for same time period were tested in compression at different loading rate and the cubes cured for different time period were tested

in terms of hardness. The results of cubes cured for same time period and tested for different loading rate are as

6.4.1 Concrete cubes tested at 40 kN/min rate of loading cured for 3 days

The concrete cubes cured in water for three days were tested in compression at 40 kN/min rate of loading and AE parameters along with I*b* value were plotted against time to study the effect of loading condition on concrete cubes cured for same time period. The AE parameters against time are as

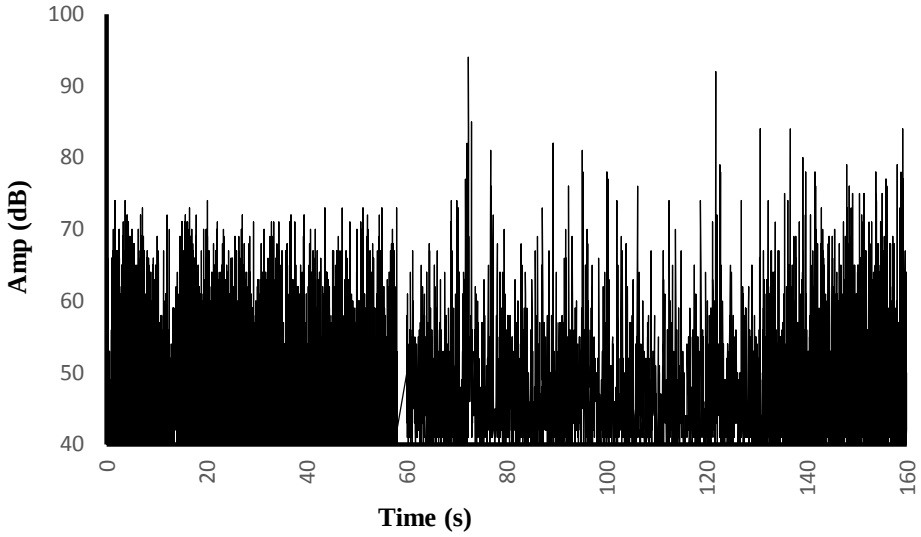

Figure 6.29 Amplitude vs time for 40 kN/min

Initially when the load was applied low magnitude AE emissions occurred. This is generally due to the presence of microvoids. As load is applied these microvoids are filled by the material surrounding them resulting in low emissions. The filling of microvoids is followed by the permanent deformation in concrete releasing high AE signals. The absolute energy is plotted against time for 40 kN/min rate of loading.

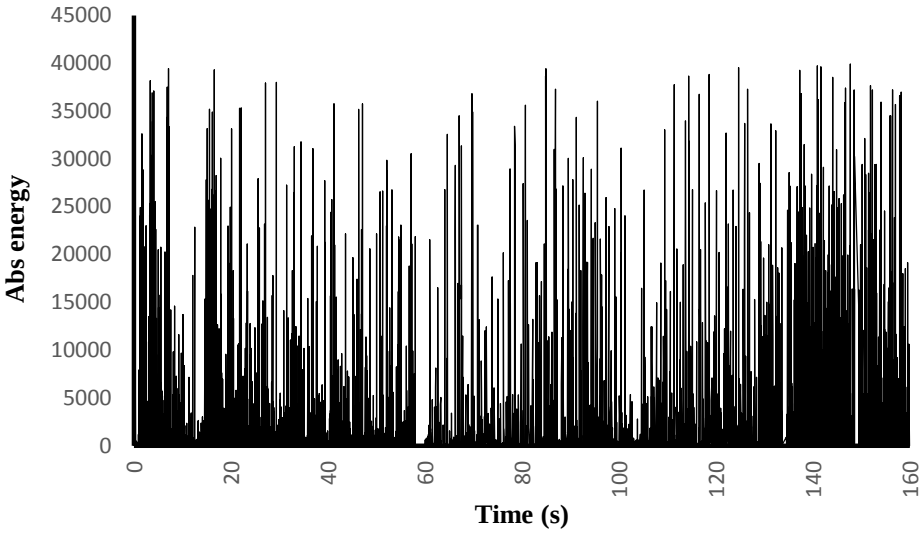

Figure 6.30 Absolute energy vs time for 40 kN/min

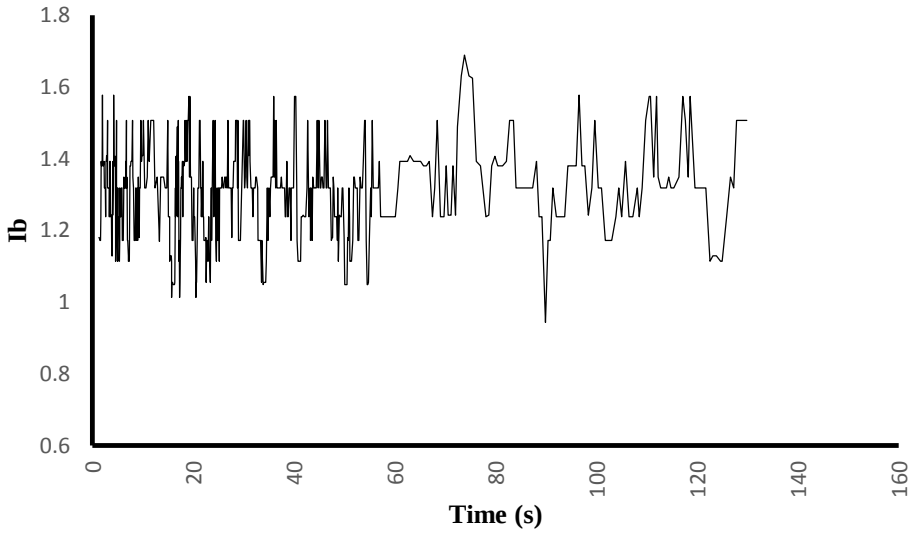

Figure 6.31 I*b* vs time for 40 kN/min

The lower I*b* value was found equal to 0.94. At this time no visible crack appeared on the surface. The lower I*b* value corresponds to internal damages occurred in the concrete specimen under compression. Then another concrete cube specimen cured for 3 days was tested at 60 kN/min rate of loading

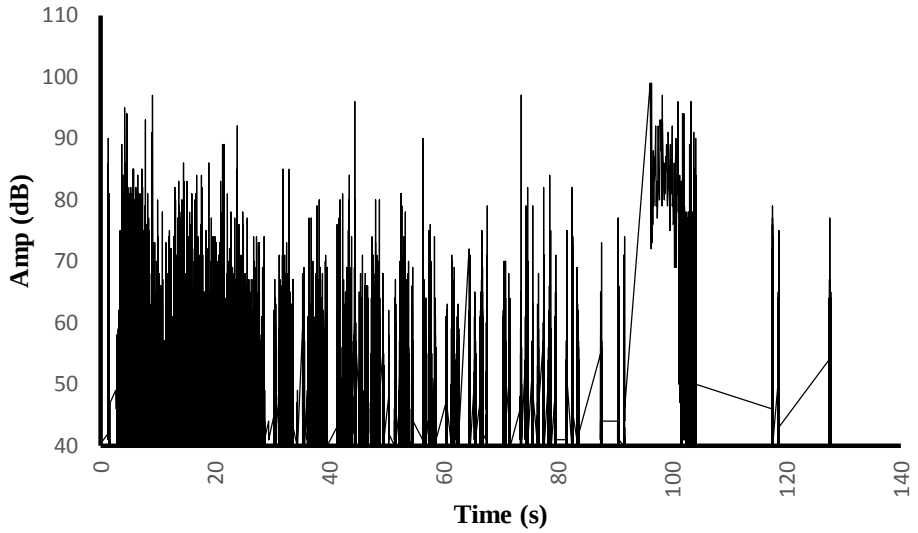

Figure 6.32 Amplitude vs time for 60 kN/min

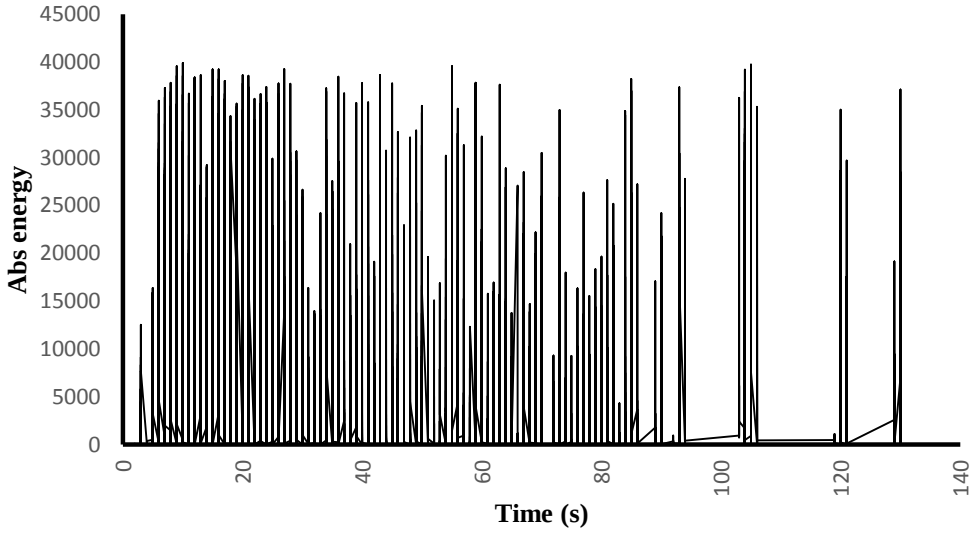

Figure 6.33 Absolute energy vs time for 60 kN/min

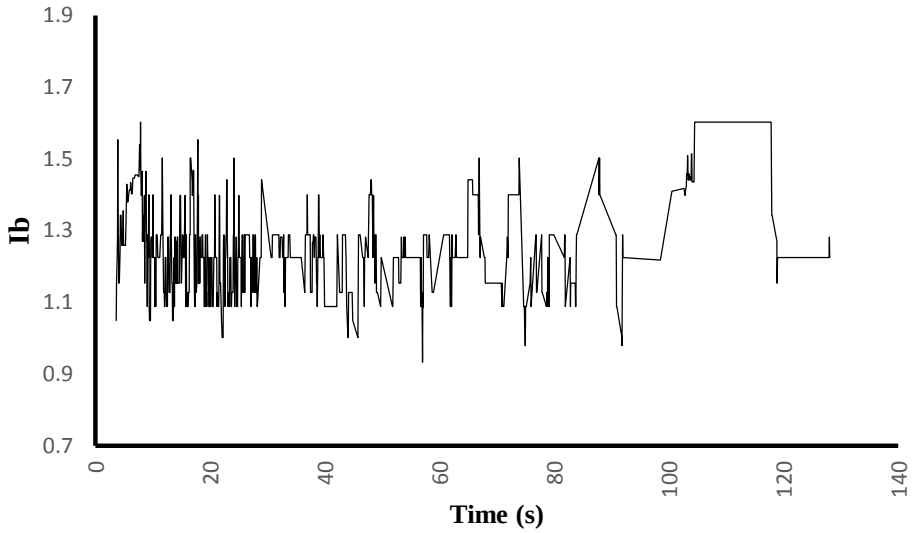

Figure 6.34 I*b* vs time for 60 kN/min

The lower I*b* value was found equal to 0.93 and was observed at time period prior to case discussed above. Thus it justifies that appearance of I*b* value is inversely proportional to the rate of loading.

6.4.3 Concrete cube tested at 60 kN/min rate of loading cured for 7 days

The load rate was then increased to 60 kN/min. The concrete specimen cured for 7 days was tested in compression at the defined loading rate. The variation of AE parameters with time is shown as

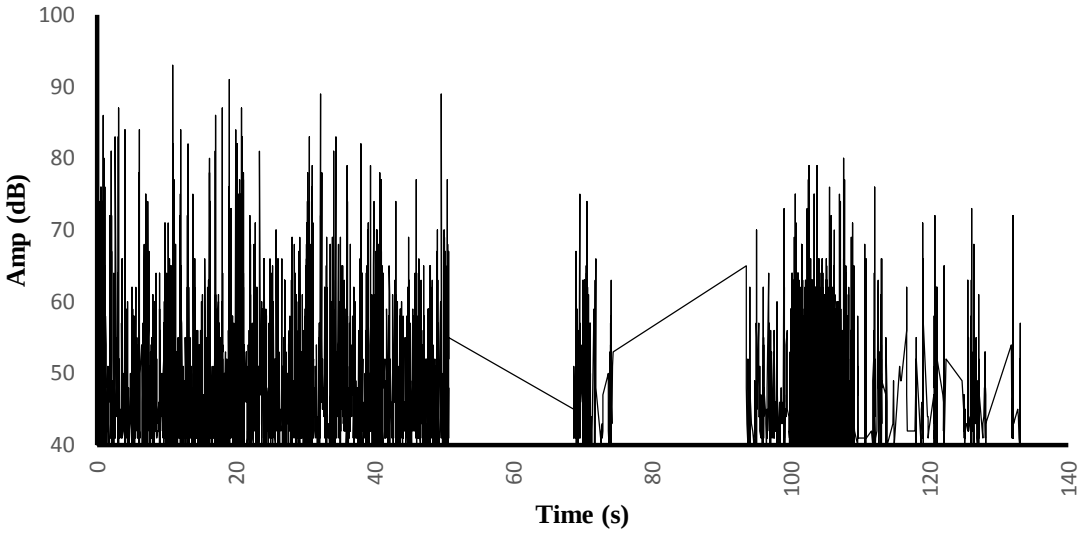

Figure 6.35 Amplitude vs time at 60 kN/min for specimen cured for 7 days

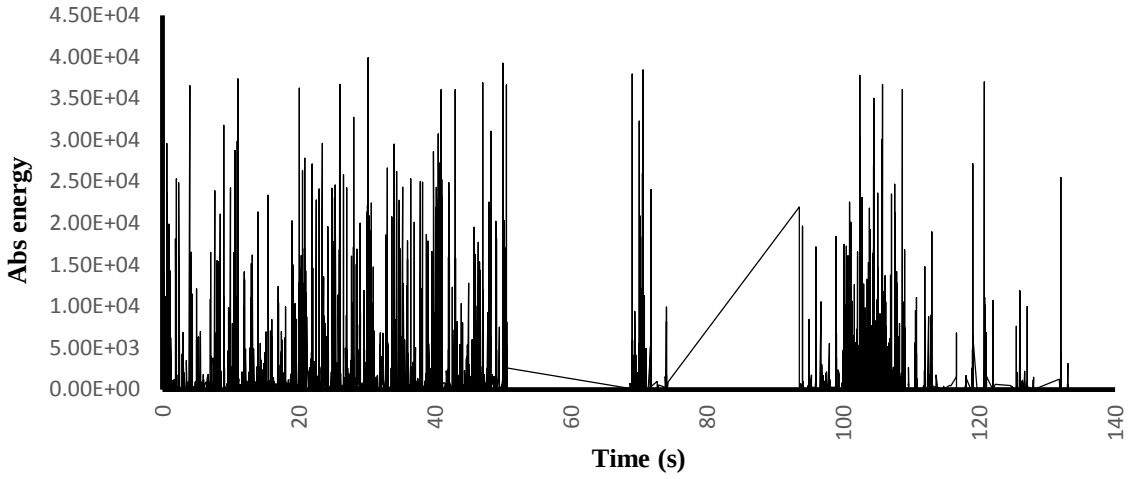

Figure 6.36 Absolute energy vs time for 60 kN/min

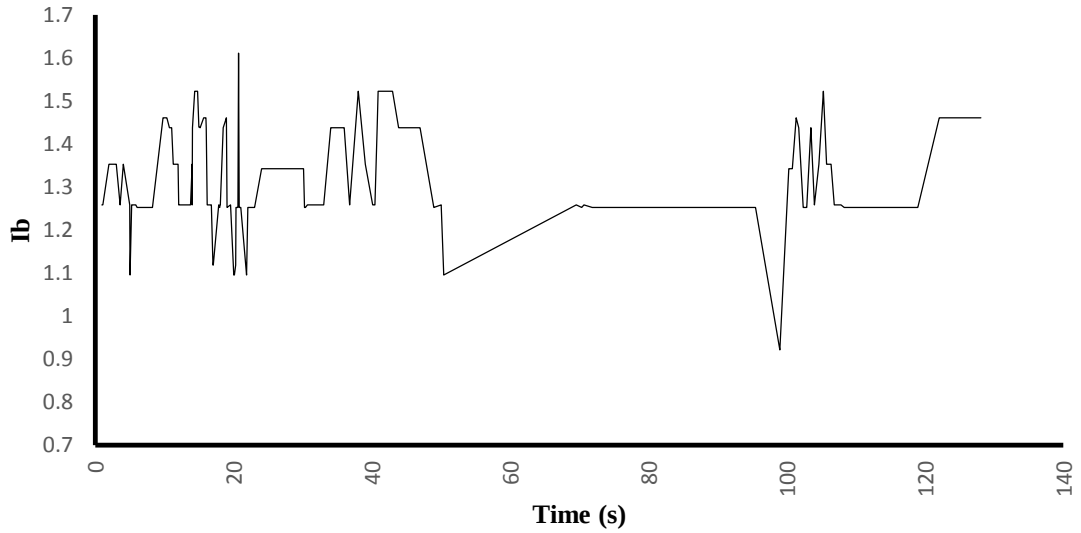

Figure 6.37 I*b* value vs time

The lower I*b* value was found equal to 0.92. The lower I*b* value appeared near 100th second which in case of 3 days curing appeared near 56th second. Thus it justifies that the strength of concrete specimen has increased with the increase in days of curing.

6.5 Conclusion and scope for further study

6.5.1 Conclusion

AE monitoring had been applied successfully to study fracture mechanism in ductile and brittle material. The effect of strain and loading rates on improved *b* value was studied in the case of ductile materials. The effect of loading rate and curing period on improved *b* value was studied

in the case of brittle materials. In the case of ductile materials, it was found that the lower I*b* value falls in the region of 0.5 to 0.7 in the transformational phase of yielding. The I*b* value was found sensitive with the varying loading rates. The lower I*b* value in the case of 30 mm/min appeared earlier than in case of lower strain rates. Similar observations were made during the three point bend test of M.S. specimen. The lower I*b* value in the case of 40 kN/min appeared earlier than in the case of lower loading rates. In the case of brittle materials, it was found that the lower I*b* value falls in the region of 0.9 to 1.2. The lower I*b* value was found sensitive with the curing period and varying load rates. The lower I*b* appearance in the case of three days curing was found earlier than in the case of seven days curing. Thus, it justifies that the strength of concrete specimen increased with increase in curing period.

6.5.2 Future scope

In present study the ductile and brittle material failure mechanism were studied. The scope for future work is listed as under

- The study can be extended to investigate failure mechanism in other materials to have valuable information of phase changes.
- The approach used in the study can be applied to real life testing of material in service. Testing in real life situations may bring extra challenges as environmental factors may contributes towards AE activity.
- A new AE setup with, installed I*b* value algorithm to calculate I*b* values can be made so that the need of calculating I*b* value from the voluminous data can be avoided.

References

[1] Farrar, Charles R., and Keith Worden. "An introduction to structural health monitoring." *Philosophical Transactions of the Royal Society of London A: Mathematical, Physical and Engineering Sciences* 365.1851 (2007): 303-315.

[2] Kumar, Dalgobind Mahto. "Recent Trends in Industrial and other Engineering Applications of Non Destructive Testing: A Review." *Global Journal of Researches In Engineering* 13.3 (2013).

[3] Hellier, Charles. "Handbook of nondestructive evaluation." (2001).

[4] Ohtsu, Masayasu. "The history and development of acoustic emission in concrete engineering." *Magazine of concrete research* 48.177 (1996): 321-330.

[5] Scruby, C. B. "An introduction to acoustic emission." *Journal of Physics E: Scientific Instruments* 20.8 (1987): 946.

[6] Lozev, Margarit G. *Acoustic emission monitoring of steel bridge members*. No. FHWA/VTRC 97-R13. 1997.

[7] Guidelines on use of acoustic emission technique, BS standard 104, 2009.

[8] Wang, K. K., G. R. Reif, and S. H. Oh. "In-process quality detection of friction welds using acoustic emission techniques." *WELDING J.* 61.9 (1982): 312.

[9] Finlayson, Richard D., et al. "Health monitoring of aerospace structures with acoustic emission and acousto-ultrasonics." *Insight-Wigston then Northampton*-43.3 (2001): 155-158.

[10] Colombo, Ing S., I. G. Main, and M. C. Forde. "Assessing damage of reinforced concrete beam using “b-value” analysis of acoustic emission signals." *Journal of materials in civil engineering* 15.3 (2003): 280-286.

[11] Drummond, G., J. F. Watson, and P. P. Acarnley. "Acoustic emission from wire ropes during proof load and fatigue testing." *NDT & E International* 40.1 (2007): 94-101.

[12] Kurz, Jochen H., et al. "Stress drop and stress redistribution in concrete quantified over time by the b-value analysis." *Structural Health Monitoring* 5.1 (2006): 69-81.

[13] Loutas, T. H., et al. "Condition monitoring of a single-stage gearbox with artificially induced gear cracks utilizing on-line vibration and acoustic emission measurements." *Applied Acoustics* 70.9 (2009): 1148-1159.

[14] Proverbio, E., V. Venturi, and G. Campanella. "Damage assessment in post-tensioned concrete viaduct by b-and Ib-value analysis of AE signal." *Proc. of NDTCE'09 Non-Destructive Testing in Civil Engineering* (2009).

[15] Kaphle, Manindra R., et al. "Damage quantification techniques in acoustic emission monitoring." (2011).

[16] Gomes, F. P. C., et al. "Evaluating the influence of contacting fluids on polyethylene using acoustic emissions analysis." *Polymer Testing* 39 (2014): 61-69.

[17] Haneef, Thodamrakandy, et al. "Study of the tensile behavior of AISI type 316 stainless steel using acoustic emission and infrared thermography techniques."*Journal of Materials Research and Technology* (2015).

[18] Mostafapour, A., and S. Davoodi. "A theoretical and experimental study on acoustic signals caused by leakage in buried gas-filled pipe." *Applied Acoustics* 87 (2015): 1-8.

[19] Sagar, R. Vidya, and M. V. M. S. Rao. "An experimental study on loading rate effect on acoustic emission based b-values related to reinforced concrete fracture." *Construction and Building Materials* 70 (2014): 460-472.

[20] Chen, Zhi, et al. "Damage analysis of FRP/steel composite plates using acoustic emission." *Pacific Science Review* (2015).

[21] Chuluunbat, Turbadrakh, et al. "Influence of loading conditions during tensile testing on acoustic emission." (2015): 121.

[22] https://en.wikipedia.org/wiki/Kadalundi_train_disaster

[23] https://www.nded.org/EducationResources/CommunityCollege/Other%20Methods/AE/E_Intro.htm

[24] https://www.nded.org/EducationResources/CommunityCollege/Other%20Methods/AE/AE_History.htm

[25] https://www.googleimages.com

[26] http://www.vallen.de/products/sensors

[27] http://www.epandt.com/images/pream024.jpg

[28] http://www.physicalacoustics.com/by-product/micro-ii/